Studying the growth and cloud activation of sodium decanoate and sodium chloride particles as surrogates of organic marine aerosols

Lauri V. Samuli Keränen

M.Sc. thesis
Physics degree programme
University of Oulu
2022

Acknowledgements

Special thanks to my lovely supervisors Silvia Calderón (FMI, Kuopio) and Jussi Malila (U. Oulu) who have helped me tremendously throughout the whole process.

Abstract

Aerosol particles transform into cloud condensation nuclei (CCN) above a critical value of the ambient water vapor supersaturation. Global climate models (GCMs) use parameterizations to estimate number concentrations of these CCN in clouds. Surfactants are organic compounds that can affect the droplet growth by e.g., decreasing surface tension of the droplet. Marine aerosols could contain an unaccounted amount of these kind of surfactants. Surfactant induced effects should be considered into calculation modules of droplet activation, droplet growth and droplet light extinction. In this thesis the cloud droplet activation of surfactant enriched aerosols is evaluated with the "simple" Köhler model (Köhler, 1936) and Köhler model combined with the monolayer model (Malila & Prisle, 2018) for surface thermodynamics. The main goal was the assessment of a modelling framework that accounts for complex surfactant effects on the droplet activation of sodium decanoate/sodium chloride particles as surrogates of marine aerosols.

It is questioned that the estimations of the cloud forming potential of secondary marine aerosols with the conventional setting of the Köhler model could be misled by using the corrected water mole fraction as a measure of the water activity.

The new composition-dependent parametrizations of water activity and density including micelles we used show a different perspective of the activation efficiency of surfactant-enriched aerosols. Even when these are surrogates of primary marine aerosols (enriched in NaCl not in SO_4 as the secondary marine aerosols), the interaction organic/inorganic controlling the surfactant behavior are very similar.

The study confirmed that the critical radius of particles values varies between 20 nm – 150 nm in normal conditions but activated droplets can be as small as 10 nm – 15 nm in radius. Our calculations agree with the results from previous studies as both models predict the minimum critical particle radius to be around 15 nm – 70 nm.

The more particles there are taking up water in the cloud the less likely it gets for an individual droplet to become a CCN. This would result in a decrease in precipitation. Our study gives insight to what is to be expected when using the conventional Köhler models for predicting aerosol-cloud interactions in marine environments. More precise and computationally efficient ways of property calculation are needed to understand the role of biogenic aerosols in the radiative forcing of marine clouds.

Contents

List of figures

Nomenclature

A	Kelvin term of the Köhler equation	m
B	Raoult term of the Köhler equation	m^3
$p_w(d_p)$	Water vapor pressure over the droplet of diameter d_p	Pa
d_p	Dry particle radius	m
$p°$	Water vapor partial pressure over the solution	Pa
$\mu_1^o(l)$	The chemical potential	J/kg
R	Universal gas constant	J/(K·mol)
T	Temperature	K
σ	Surface tension	N/m
ρ_i	Density of species i	kg/m^3
S	Saturation ratio	
δ	Surface thickness	Å

Introduction

Aerosol particles, which are solid or liquid matter suspended in the atmosphere, play a role in the process of cloud formation as well as in the radiative balance of Earth. They have a direct interaction with the solar radiation by absorption and scattering accounted for as the effective radiative forcing due to aerosol-radiation interactions, ERF_{ari}. Aerosol particles can also act as seeds for water condensation and affecting the number and size of nascent cloud droplets known as cloud condensation nuclei (CCN). Aerosol particles modify the cloud albedo effect and the cloud lifetime. Their indirect effects on the solar radiation balance are accounted for as the effective radiative forcing of aerosol-cloud interactions, ERF_{aci}. Aerosol particles can be divided in subcategories; primary aerosols, which are emitted directly from a source to the atmosphere or secondary aerosols, which are formed from gas-to particle conversions in the atmosphere. These particles can either come from natural sources (oceans, deserts, forests) or anthropogenic sources which are human-induced (traffic or industrial emissions) (IPCC, 2014; Seinfeld & Pandis, 1998a).

Aerosol particles transform into cloud condensation nuclei (CCN) above a critical value of the ambient water vapor supersaturation. If this limiting value, referred as activation point, is exceeded inside an air parcel, the droplet spontaneously grows and becomes a cloud droplet. The properties of the particles can affect the activation point. Particle size, concentration and chemical composition are the main ones, and they can change because of condensation, evaporation, coagulation and chemical reactions in the atmosphere (Seinfeld & Pandis, 1998b).

Global climate models (GCMs) use parameterizations to estimate number concentrations of CCNs based on aerosol number concentrations, size distributions and inputs related to the thermodynamic state of the atmosphere such as vertical updraft, temperature and relative humidity. Although the most advanced activation schemes take into account the effect of water-soluble organic compounds on water activity through the κ-value or effective hygroscopicity parameter (e.g. global ECHAM/MESSy Atmospheric Chemistry, EMAC (Chang et al., 2017)), the effect of surfactants has not been explicitly accounted for (Abdul-Razzak & Ghan, 2004).

Surfactants are organic compounds that have the tendency to move to the solution–air interface because of their dual chemical nature which has a hydrophilic and a hydrophobic part (Langevin, 1992a). The presence of surfactants in aerosol particles can affect droplet growth by decreasing the surface tension of the droplet solution below the value of the pure water (Z. Li et al., 1998) and by changing the water activity of the droplet bulk solution after experiencing bulk–surface

partitioning as evidenced by both, experiments and theory (Bzdek et al., 2020; Sorjamaa et al., 2004). Since current models do not include these effects on the formation of cloud condensation nuclei, more precise predictions and models are needed to reduce the uncertainty of aerosol-induced radiative forcing in GCMs (Nenes et al., 2001; Nenes & Seinfeld, 2003).

The variety of organic substances of atmospheric relevance that could behave as surfactants makes their chemical characterization very difficult to achieve (Nozière et al., 2017a). However, aqueous extracts of aerosol samples and cloud/rainwater samples collected from diverse environments have shown low surface tension values as those observed for aqueous surfactant solutions (Asa-Awuku et al., 2008; Dinar et al., 2006; Ekström et al., 2010; Facchini et al., 1999, 2000; Gérard, Kumar Singh, Dharmendra Fine, et al., 2019; Kiss et al., 2005; Kroflič et al., 2018; Mochida et al., 2002; Nozière et al., 2017; Renard et al., 2016, 2019). Recently, Renard et al. (2019a) characterized a series of surfactants produced by microbial strains isolated from cloud water samples. These findings have revived the old discussion about the important role that microorganisms such as bacteria, fungi and yeast could have effect in aerosol activation to cloud droplets or ice crystals (Burrows et al., 2009a; Delort et al., 2010).

The sea surface has been pointed out as significant source of these surfactants of biological origin, referred as biosurfactants, can be produced by phytoplankton, cyanobacteria and several seaweeds (O'Dowd et al., 2004; Oppo et al., 1999). With increasing supporting evidence, it is believed that these biosurfactants enrich the sea surface layer and participate actively in the production of primary marine aerosols via bubble bursting (Burdette & Frossard, 2021; Frossard et al., 2019) and also in the production of secondary marine aerosols via ozonolysis for example the oxidation of fatty acids (Alpert et al., 2017; Lawler et al., 2020).

Under the scientific premises that marine aerosols are the biggest contributors to aerosol loadings at global scale (IPCC et al., 2021) and that they could contain an unaccounted amount of surfactants with significant influence on the radiative forcing of aerosols and clouds, we support the hypothesis that it is essential to understand how surfactants affect the air–droplet interface because of surfactants potential ability to 1) modify the water uptake and the cloud forming potential of inorganic aerosols, and 2) modify the size of CCN and the composition of the droplet surface and therefore, the refractive index of cloud droplets.

Nonetheless, testing this multi-angle perspective hypothesis in global climate models is a challenging task, if not impossible, with current modelling frameworks. Surfactant induced effects should be considered into calculation modules of droplet activation, droplet growth and droplet light extinction. For every droplet size change, every module must include an extra step to resolve the variation of the composition of the droplet bulk solution due to bulk–surface partitioning. This process

can increase the computing time to unreasonable limits as the equations are highly nonlinear and must be numerically solved per every combination of droplet size and composition.

This thesis

In this thesis the cloud droplet activation of surfactant enriched aerosols is evaluated with the Köhler model (Kohler & Köhler, 1936) and the monolayer model (Malila & Prisle, 2018). The activation point of dry particles is formed by a fatty acid sodium salt and sodium chloride, as surrogate of marine aerosols using bulk–surface (B/S) partitioning models. CCN activation of organic aerosols in atmospheric chemistry-climate models are based on the hygroscopicity parameter through the κ–Köhler theory. They may incorrectly calculate surfactant-induced effects such as bulk-surface partitioning, surface tension depression and more important, the surfactant aggregation or micellization. The effect of water-soluble organic compounds on water activity is included in most GCMs cloud activation processes via the κ-Köhler theory (Petters & Kreidenweis, 2007), however CCN values can also be affected by changes in the surface tension of the droplet solution at activation induced by surfactants. In this thesis we calculated the activation point of dry particles, formed by a fatty acid sodium salt and sodium chloride, as a surrogate of marine aerosols using B/S (bulk–surface) partitioning models. Different B/S models offer a different representation of the dimensionality of the droplet surface and based on the same inputs of dry particle diameter and organic mass fraction, calculate the critical radius and critical saturation that correspond to the activated droplet. In the first modelling approach based on the simple Köhler model, surfactant effects on the water activity are accounted for using an activity coefficient model with specific treatment for solution nonidealities derived from surfactant aggregation. In the second approach based on the monolayer model, besides the activity coefficient model, composition-dependent parametrizations of the density and surface tension in surfactant/inorganic salt aqueous solutions are utilized to estimate the monolayer thickness during bulk-surface partitioning calculations.

The main goals for the thesis are:

1. Investigate the cloud activation potential of secondary marine aerosol surrogates with full consideration of solution nonidealities and micelle formation into a bulk–surface partitioning scheme.

2. Assess possible biases in droplet growth, critical supersaturation, and critical diameter when a conventional Köhler calculation is used (this means the use of the Köhler model with no partitioning and water activity calculated as the corrected molar fraction)
3. Explore the possibility of having micelles in activated droplets or interstitial aerosols in atmospheric conditions like those of marine clouds.

To the best of our knowledge, this is the first study that considers solution nonidealities into the droplet activation of sodium decanoate–sodium chloride aerosol particles with explicit description of the inorganic salts' effects on the surfactant adsorption via composition-dependent parameterizations of critical micelle concentration, water activity, solution density and surface tension.

Theoretical framework

Köhler theory

Developed by Hilding Köhler in the early 20th century his theory defines the conditions to reach thermodynamic equilibrium for water at an air–liquid interface and provides a method to evaluate the activation of particles to form cloud droplets (Köhler, 1936). Köhler theory is often used as a basis for parametric description of cloud formation in GCMs.

In its classical form, the Köhler theory assumes a very diluted droplet solution where the surface tension and the partial molar volume of water are equal to those of pure water, the volume occupied by solute molecules is negligible compared to the total droplet volume, the water activity coefficient is equal to unity and the logarithm of the saturation ratio of water can be approximated to the first term of its Taylor series.

Under these assumptions, the parametrization of the cloud activation in terms of the critical saturation S_c and the critical radius R_c of an activating droplet is given as (Seinfeld & Pandis 2016)

$$\ln\left(\frac{p_w(d_p)}{p^\circ}\right) = \frac{A}{d_p} - \frac{B}{(d_p)^3}, \qquad \text{Eq. 1}$$

where $p_w(d_p)$ is the water vapor pressure over the droplet of diameter d_p, p° is the water vapor partial pressure over the solution, and the coefficients *A* and *B* are defined as follow

$$A = \frac{4\sigma M_w}{RT\rho_w}, \qquad B = \frac{6n_s M_w}{\pi\rho_w}, \qquad \text{Eq. 2}$$

where σ is the surface tension of the solution, M_w is the molar mass of water, R is the universal gas constant, T is the temperature, ρ_w is the density of water and n_s is the amount of moles of the solute in the solution.

The coefficient *A* comprises variables involved in the so-called Kelvin effect which describes the effect of curvature to the vapor pressure of the solution, as the saturation vapor pressure of a curved surface is always larger than the one of a flat surfaces. The coefficient *B* comprises variables involved in the so called Raoult effect which describes the influence of the solute partial pressure of water decreases when the solute concentration increases (Köhler, 1936). On smaller droplets the

Kelvin term dominates and on larger ones the Raoult term is the dominant one, though both increase with decreasing droplet size.

The effect of the two terms can be seen in Fig.1. As the droplet radius D_{wet} decreases, both the solute effect (Raoult) and the curvature term (Kelvin) increase. But as it can be seen the Raoult term increases much faster. The Köhler curve, which is the result of interaction between the two terms gives us the amount of saturation of water in the surroundings needed to make the droplet grow. The critical point in the curve, seen as a dot in Fig.1, gives us the maximum of the needed supersaturation for the droplet to grow spontaneously. If the supersaturation is lower than the critical supersaturation, the droplet does not have enough water vapor for it to become a CCN and will evaporate completely due to the unstable nature of pure water droplets.

Without consideration of surface tension effects, the surface tension is always equal to the surface tension of pure water. All particles share the same curve of the Kelvin effect (red) and differences in their Köhler curves are defined by the Raoult effect, which depends on the total amount of solute in the droplet solution and the solution nonidealities (i.e. water activity). It is commonly assumed that solution nonidealities can be disregarded as droplets are considerably diluted under supersaturated conditions (Nenes et al., 2001). When solutes are strong electrolytes such as sodium chloride (NaCl) it is assumed that the water activity is proportional to the effective molar fraction of water that accounts for solute dissociation (i.e. each NaCl molecule dissociates into a sodium ion (Na^+) and a chloride anion (Cl^-) doubling the total number of solutes in solution). This representation of water activity is preferred in CCN parameterizations (Abdul-Razzak & Ghan, 2000).

Under this assumption, Fig. 1 shows how the curves of the Raoult effects of dry particles of 20 nm and 80 nm are very similar in shape but displaced due to the higher mass of the larger particle. Differences in their Köhler curves and activation points are basically consequence of the curvature-enhanced vapor pressure over the smaller droplets. An activated droplet will be ten times larger in this case, and the large dry particle will be easier to activate in milder conditions. The growth factor of an 80 nm droplet is significantly larger than the one for the 20nm droplet. This means the activating droplet is significantly larger compared to the dry particle.

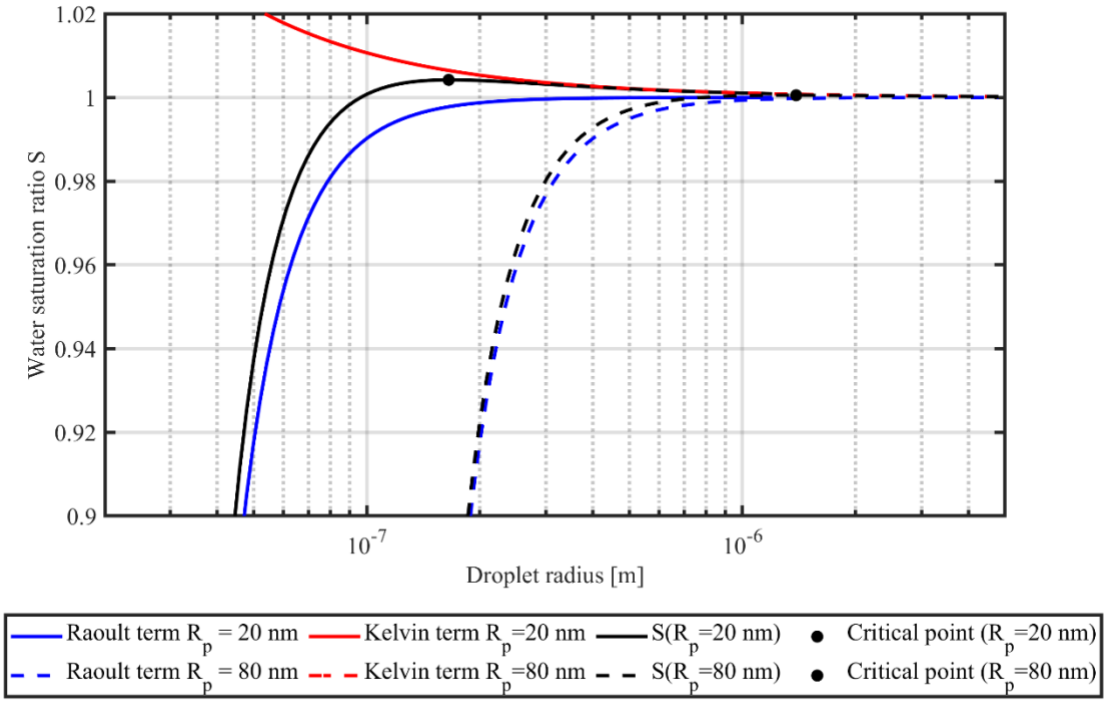

Figure 1 Köhler curves for dry particles composed of sodium chloride (NaCl) with radius of 20 nm and 80 nm. Water saturation ratio (S) over droplet surface is defined as the product of both, the Raoult term and the Kelvin term, shown separately. The global maximum of the water saturation ratio is referred as critical point.

Formation of droplets in the atmosphere

A pure water droplet in the atmosphere is unstable, meaning a small perturbation in the droplet (evaporation or condensation) is sufficient to complete evaporation or uncontrollable growth. In the atmosphere there are practically always particles for the water vapor to condensate on, making such behavior unlikely. The process of cloud formation is modeled through the variation of the water saturation (S) inside a rising parcel of air that expands adiabatically. Figure 2 shows the temporal variation of S in the air parcel compared to the Köhler curve of three different aerosol particles with activation points defined by critical saturation values of S_{c1}, S_{c2} and S_{c3}. When the cloud formation starts, the saturation increases rapidly reaching a maximum value that depends on both, the thermodynamic state of the atmosphere (i.e. temperature, total water specific content) and the condensation sink represented by aerosol particles. Even when all aerosol particles require a critical saturation that is below the maximum saturation in the air parcel, just the aerosol particle

corresponding to the yellow activates when $S > S_{c3}$ and continuously grows to become a stable cloud droplet as its equilibrium saturation is always lower than the saturation of the air parcel. Other Köhler curves indicate that droplet activation never occurs (red and blue curves), but then evaporation effects limit the droplet growth (green curve). This indicates that droplet activation cannot be completely understood without considering the dynamics of the atmosphere (Nenes et al., 2001).

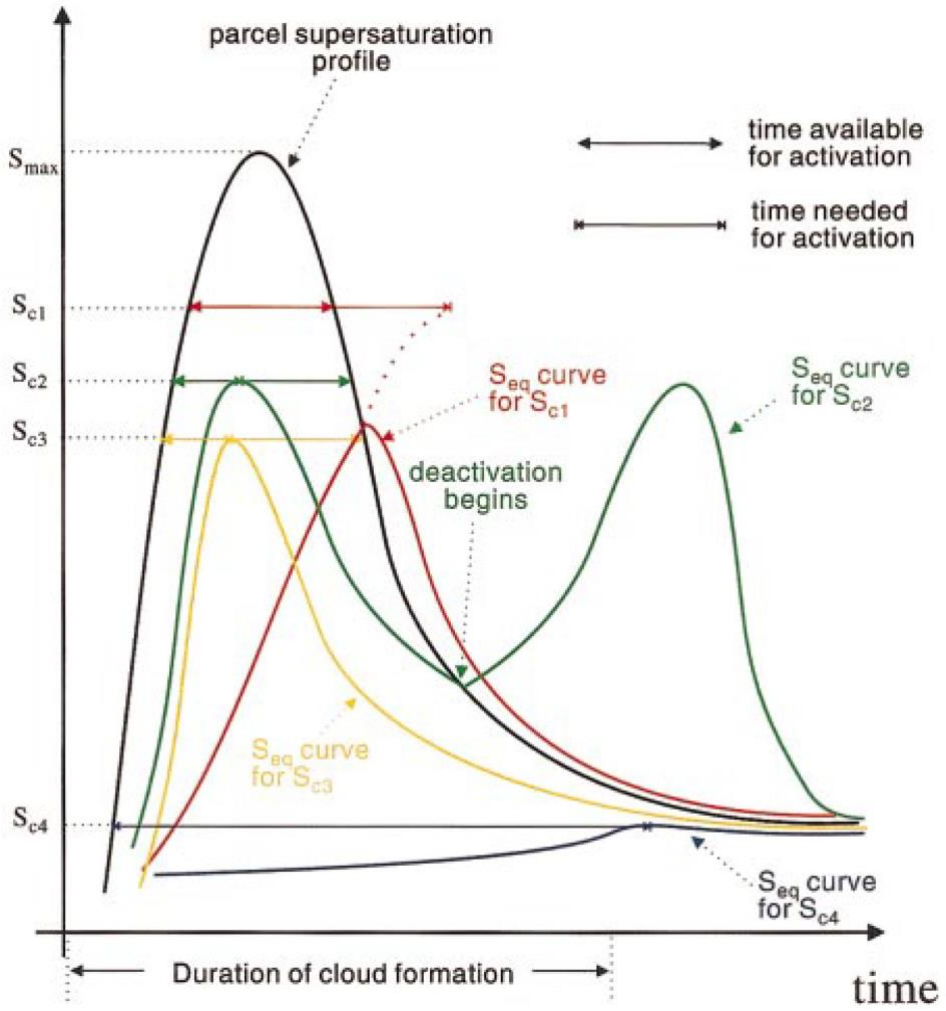

Figure 2 Droplet activation inside an adiabatic cloud parcel Athanasios Nenes, Steven Ghan, Hayder Abdul-Razzak, Patrick Y. Chuang & John H. Seinfeld (2001) Kinetic limitations on cloud droplet formation and impact on cloud albedo, Tellus B: Chemical and Physical Meteorology, 53:2, 133-149, DOI:10.3402/tellusb.v53i2.16569 http://creativecommons.org/licences/by/4.0/

Surfactants

A surfactant is an abbreviation from SURFace ACTive AgeNT (Clint, 1992) used to refer those organic molecules with hydrophobic and hydrophilic moieties that show surface activity, which means that they tend to accumulate on the surface of a liquid or at the interface of two phases changing the properties of the bulk solution, such as surface tension. The hydrophilic or soluble part of the surfactant can be charged to an extent, and the hydrophobic or insoluble part is more often free of charge. The insoluble part does not have significant interaction with water molecules, but the ionic part does via dipole or ion–dipole interactions (Romsted, 2012a). In an aqueous solution, water molecules repel this insoluble part consisting usually out of a hydrocarbon chain, and both, dispersion and hydrogen bonding forces drive the compound to accumulate on interfaces (Tharwat, 2014).

Surfactants can be ionic and nonionic depending on their degree of dissociation in aqueous solution. As an example of an ionic surfactant, Figure 3 shows the molecule of sodium decanoate ($CH_3(CH_2)_8COONa$) that dissociates in water by releasing the sodium ion. After dissociation, the decanoate ion is formed by the hydrophilic part comprised by the acetate ion (COO^-) and the hydrophobic part comprised by the long chain of nine methyl groups. When the interface is saturated and cannot adsorb more surfactant molecules, they accumulate in the bulk solution and start to form aggregates called micelles. Micelles can change their shape and size depending on the surfactant concentration in solution but are also sensitive to the presence of other surfactants or inorganic salts (Langevin, 1992b). Figure 4 shows a schematic description of a spherical micelle inside an aqueous solution. Driven by their chemical affinity, surfactant molecules come together pointing their hydrophilic parts towards the bulk solution while hydrocarbon tails accumulate to the center of the micelle (Tharwat, 2014).

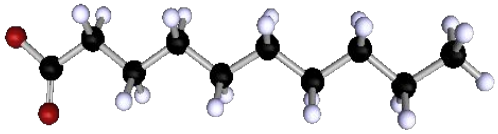

Figure 3 Schematic representation of the sodium decanoate molecular structure. The hydrophobic tail composed of carbon atoms (black) and hydrogen atoms (white) is connected to the hydrophilic head that comprises the acetate group containing an oxygen atom (red)

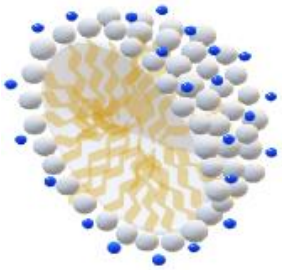

Figure 4 Schematic representation of the organization inside micelle in aqueous media. Surfactant molecules form an aggregate with their hydrophilic parts oriented towards the aqueous solution and their hydrophobic parts towards the inner part.

Surfactant adsorption at the air-droplet interface

While increasing the amount of surfactant in the solution, the surface tension at the air-solution interface is depressed. This is as the surfactant partitions to the surface and arranges itself spontaneously. The decrease in the surface tension comes from the diminished intermolecular forces between the surfactant molecules compared to water molecules (Romsted, 2012b). Partitioning is driven by diffusion from the bulk to the surface and how the molecules transfer to the interface.

Surfactant adsorption can be followed using the variation in the solution surface tension induced by increasing surfactant concentration as shown in Figure 5. Pure water surface tension is $72.8\ \mathrm{mN/m}$, at $20°\ \mathrm{C}$ (Petrova & Dooley, 2014) and starts to decrease as the amount of surfactant in solution is increased. Molecules organize in the surface pointing their hydrophobic tails towards the air side. With increasing surfactant concentration, the adsorption increases until the surface is saturated and cannot take more surfactant molecules. At this point, referred as Critical Micelle Concentration (CMC), there is thermodynamic equilibrium between monomers in the bulk solution and the monomers at the surface (Shinoda & Hutchinson, 1962). At concentrations above the CMC, the surfactant adsorption cannot longer occur at the surface, excess molecules stay on the bulk

solution and start to experience self-aggregation. The common technique for measuring the CMC is through surface tension which abruptly changes at CMC and remains virtually constant when the concentration is further increased. Other observable changes in solution properties related to the CMC include increasing turbidity, decreasing NMR self-diffusion, conductivity and electrical potentials. (Romsted, 2012b)

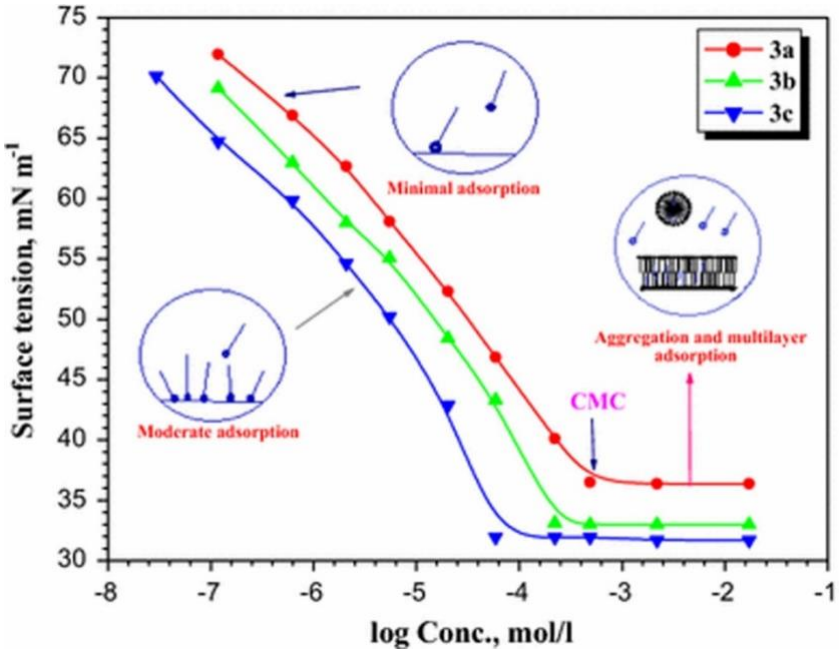

Figure 5 Changes induced by surfactant adsorption in the surface tension of an aqueous solution as function of the surfactant concentration. Abd El-Lateef, H. M., Tantawy, A. H., & Abdelhamid, A. A. (2017). Novel Quaternary Ammonium-Based Cationic Surfactants: Synthesis, Surface Activity and Evaluation as Corrosion Inhibitors for C1018 Carbon Steel in Acidic Chloride Solution. *Journal of Surfactants and Detergents*, *20*(3), 735–753. https://doi.org/https://doi.org/10.1007/s11743-017-1947-7. Copyright © 1999-2022 John Wiley & Sons, Inc., reprinted with the permission of the publisher."(Abd El-Lateef et al., 2017)

Aggregation can be affected by temperature and/or addition of salts, organics or other surfactants. The surfactant can appear in several aggregate structures depending on the composition of the solution (Romsted, 2012a). Inorganic salts tend to increase the surface tension of aqueous solutions, while some organic salts can behave as surfactants (Pegram & Record, 2007; Romsted, 2012b). In marine environments the most consistent compounds are sea salts that increase the surface tension of aqueous solutions as the salinity is increased (Vinš et al., 2019).

The micellization of surfactants has been studied previously, but not extensively the implementation to models in modeling the properties of aerosol particles. Recently (Calderón et al., 2020c) presented a model for estimating the activity coefficients in binary and ternary ionic surfactant solutions. Also, for the density of the droplets a model that considers the effect that micellization has in atmospheric droplet model solutions (Calderón & Prisle, 2021).

Surfactants of atmospheric relevance

Surfactants have been detected in aqueous extracts from atmospheric aerosols at all size-ranges (Gérard, Noziere, et al., 2019; Kroflič et al., 2018) and also in cloud water samples (Renard et al., 2019). Surfactants in the atmosphere can originate from man-made sources, they have been found in emissions from cooking, biomass burning, fossil fuel combustion (Renard et al., 2016) or generated by oxidation and photooxidation of semi volatile organic compounds (Alpert et al., 2017). Figure 6 shows examples of surface-active molecules produced by oxidation of organo-sulphates in the atmosphere (Hyttinen et al., 2020). They can also be naturally produced by a wide range of microorganisms present in soil, seawater and sediments. Global emissions of bacteria-containing particles from grasslands, shrubs and crops are in the order of $7.6 \times 10^{23} – 3.5 \times 10^{24}$ $1/a^{-1}$ representing approximately a total mass of emitted bacteria of 40 Gg–1800 Gg y^{-1} (Burrows et al., 2009). Bacteria are expected to exist in micron and submicron particles having longer atmospheric residence times up to 1 or 2 weeks that may allow them to travel up to thousands of kilometers (Burrows et al., 2009b; Després et al., 2012; Ogunro et al., 2015). Atmospheric particles containing bacteria show a counter median diameter between 2 μm and 4 μm (Burrows et al., 2009), and concentrations of bacteria in cloud water are in the order of 10^5 mL^{-1} (Gerard et al. 2019). Bacteria such as the *Pseudomonas sp.* PDD-14b-2 produce metabolites with very strong surface-activity such as the viscosin-A molecule shown in Figure 9, recently derived from cloud water samples and chemically characterized (Renard et al., 2019). This type of surfactants is referred as biosurfactant. According to (Gerard, 2017, p.18) there are six major biosurfactant classes: glycolipids, lipopeptides/lipoproteins, phospholipids, neutral lipids, fatty acids and lipopolysaccharides. Polysaccharides and long chain fatty-acids show decreased hygroscopicity compared to free saccharides (Cochran et al., 2017). Compared to the sodium decanoate molecule in Figure 3, biosurfactants such as viscosin-A in Figure 7, are more efficient regarding their ability to reduce the surface tension of aqueous solutions, as a much lower concentration is needed to decrease one unit of surface tension.

The preferential adsorption of surfactants at the air-droplet interface shifts the properties of the droplet bulk solution increasing the water activity in Eq. 1 from the value obtained at total composition (Prisle et al., 2010). At large concentrations, cloud droplet activation can occur with a significant reduction of the surface tension of the droplet solution from the value of pure water (Ovadnevaite et al., 2017), typically assumed for calculations of the critical supersaturation performed

with Eq. 1 and Eq. 2. In addition, the droplet surface solution becomes enriched in the surfactant and shows different optical properties (Bzdek et al., 2020). Significant reduction of the critical activation diameter of inorganic seed particles coated with surfactants have been observed in chamber experiments (Sareen et al., 2013).

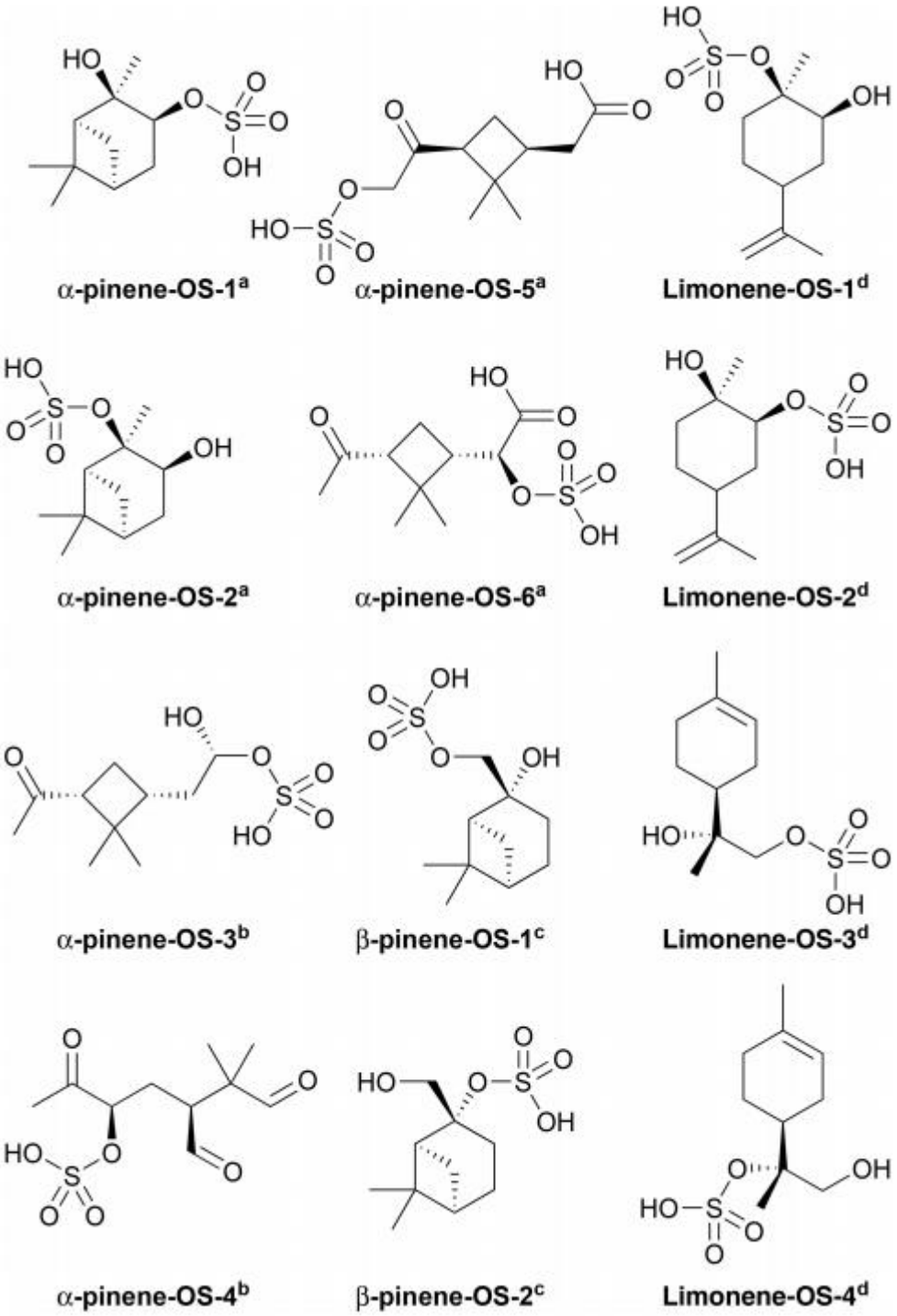

Figure 6 Organic compounds found in atmospheric aerosols with surface-active behavior in aqueous solutions. https://creativecommons.org/licenses/by/4.0/ (Hyttinen et al., 2020a)

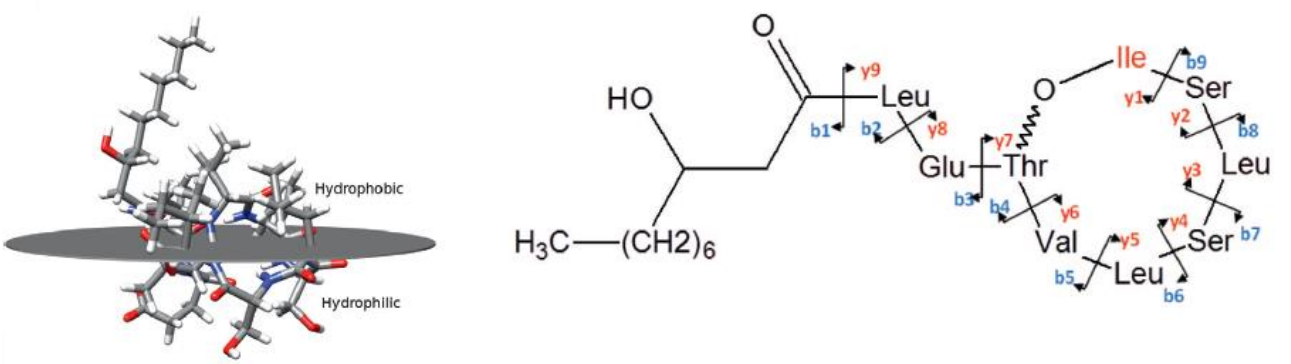

Figure 7 Viscosin, as an example of a biosurfactant found in cloud droplets and rain water. Leu, Glu, Thr, Ser and Val refer to segments of the following substances leucine, glutamic acid, serine and valine (http://creativecommons.org/licenses/ by/3.0) (Renard et al., 2019)

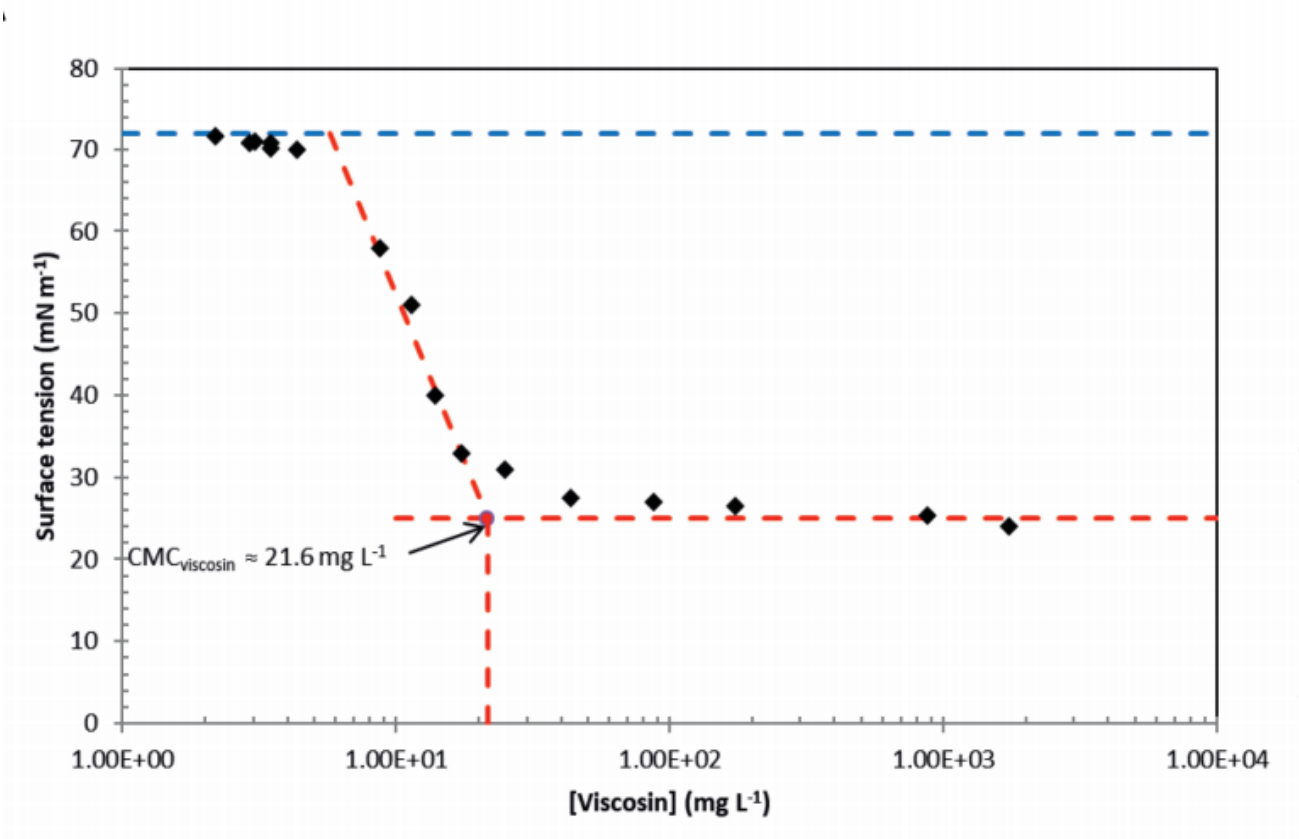

Figure 8 Surface tension of aqueous solutions containing viscosin and estimated critical micelle concentration (CMC) (http://creativecommons.org/licenses/ by/3.0) (Renard et al., 2019)

Surfactants in marine aerosols

There have not been studies of specific, accurate chemical classification of surfactants in marine environments. Sea surface surfactants are most often referred with their ionic nature, or a chemical hypernym, as there is a vast number of compounds with surface active properties in the sea surface. (Floris et al., 2020) Though this is most often practical for the sake of the studies in hand, this kind of study would be beneficial to model the properties more accurately.

Sea spray aerosols are an important factor in climate systems by being the main contributor to light scattering in the marine boundary layer. This is a huge effect considering the amount of sea surface on earth and is considered one of the most important components of natural aerosols that are able of affecting the Earth's radiative balance (De Leeuw et al., 2011; Quinn et al., 2015). In seawater microbial activity generates substances considered biosurfactants, it is likely there are hundreds of these but there is not sufficient characterization of these yet (Schiffer et al., 2018).

It has been proposed that can be transferred to atmospheric aerosols during bubble bursting at the seawater surface (Mochida et al., 2002), and according to Kristensson et al. (2010), this phenomenon produces sea spray particles containing amino acids originating from phytoplankton in coastal areas and bacteria in more offshore environments.

Sea spray aerosols can be broken into primary sea spray aerosols (SSA) and secondary marine aerosols (SMA). SSA originate from bubble bursting on sea level (Mayer et al., 2020a). Breaking waves contain air bubbles which when the wave breaks are broken into hundreds of droplets of a broad size range. The flux is affected by wind speeds and sea surface temperature (Kasparian et al., 2017).

The particle composition can have a wide variety of substances in addition to sea salts and water. Compounds found in sea spray contain as primary aerosols polysaccharides, proteins, fatty acids, gels, microorganisms, HUMIC-like substances, amino acids and vesicles (Schiffer et al., 2018). Secondary marine aerosols are the sulfur compounds found in sea spray in the form of dimethyl sulfide (DMS). They accumulate from gas-to-particle conversion of the oxidation products of gas phase species of DMS and other biogenic volatile compounds. These secondary aerosols are found to have a dominant role in affecting marine cloud properties as they correlate with marine phytoplankton biomass unlike SSA. Also the CCN activity of SMA is close to the one observed by field studies (Mayer et al., 2020b). Hygroscopicity of the SSA is at its lowest point while heterophilic bacteria levels were greatest, revealed the CCN measurements during phytoplankton bloom experiments according to (Schiffer et al., 2018).

The amino acids can behave as effective CCN (Kristensson et al. 2010b). The experimental result of surface-active substances having effect on the surface tension of droplets was found for small droplet sizes by Li et al., (2013) in their MD simulations. They also stated the surface tension effect is considerably large in nano-sized droplets but negligible in activated droplets. As particles with sizes below 200nm in diameter will dominate the marine CCN number population, we will assume the contribution from sea salt to be insignificant relative to organic matter.

Sodium decanoate–sodium chloride composed particles are proxies for aerosol particles in a marine background. Fatty acids in the oceans have a tendency of existing in an ionic form because of the sea water pH (Prisle et al., 2008). Therefore, the generation of sodium salts of the fatty acids is expected with the loss of hydrochloric acid, as marine aerosols tend to have a major fraction of sodium salt (Prisle et al., 2008; Stephanou, 1992).

In the following section, we will go through the models used to estimate the thermodynamic properties of aqueous solutions containing sodium decanoate and sodium chloride, both referred from now on as NaDec and NaCl. Likewise, we will introduce the models used to include the effect of bulk–surface partitioning in the growth and activation of atmospheric droplets formed from our proxies of marine aerosols.

Material and methods

General properties

Droplet solutions were treated as a ternary system composed by water or compound 1, sodium decanoate as surfactant or compound 2 and sodium chloride as inorganic salt or compound 3. Properties of droplet solutions were represented as vectors, one vector component per compound. For example, droplet solution composition is represented as

$$x = [x_1, x_2, x_3] \text{ with } x_i = n_i\left(\sum_j n_j\right)^{-1} \qquad \text{Eq. 3}$$

denoting the mole fraction of species i in solution.

Table 1 shows physico-chemical properties relevant in the calculation of Köhler curves for our surrogate marine aerosol particles.

Table 1 Physico-chemical properties relevant in calculations

Property	Units	Water	Sodium Decanoate (NaDec)	Sodium Chloride (NaCl)
Compound number	-	1	2	3
Empirical formula	-	H_2O	$CH_3(CH_2)_8COONa$	NaCl
CAS number (Weast, 1989a)		7732-18-5	1002-62-6	7647-14-5
Molecular weight x 10^3 (Weast, 1989b)	kg mol^{-1}	18.0153	194.247	58.4428
Density as solid in atmospheric conditions (296 K, 1 atm) (Weast, 1989b)	kg m^{-3}	n/a	1101.61	2165.00
Density in liquid or hypothetical supercooled liquid (296 K, 1 atm) (Calderón & Prisle, 2021) (Janz, 1988)	kg m^{-3}		1101.61	1978.21
Molecular volume in liquid or hypothetical liquid state estimated from density x 10^{27}	m^3 $molecule^{-1}$	0.0300	0.2934	0.0491
Surface tension in hypothetical supercooled liquid (293 K, 1 atm) (Petrova & Dooley, 2014)	mN m^{-1}	72.8	25.864	163.873
Surface thickness of a pure monolayer estimated from molecular volume x 10^9	m	0.3855	0.8244	0.4542

Thermodynamics properties of aqueous solutions of sodium decanoate and sodium chloride

Köhler calculations require the water activity in droplet solutions, and this must be calculated with an activity coefficient model.

Thermodynamically, the activity of water is a measurement of the change in the fugacity of a compound in solution compared to its fugacity in pure state at the same temperature and pressure. It originates from the Gibbs free energy at constant temperature T and pressure p, and can be derived from:

$$\mu_1(x,T) = \mu_1^o(T) + RT\ln(a_1), \qquad \text{Eq. 4}$$

where R is the universal gas constant, μ is the chemical potential of the pure water at temperature T. In an ideal solution the water activity can be directly taken as the mole fraction of water (Blandamer et al., 2005a). In the presence of electrolytes such as NaCl, the water activity can be approached as the effective molar fraction of water that accounts for the presence of all ionic and nonionic species in solution.

The water activity can be related to the osmotic coefficient and to the ion activity coefficient by the link created by the Gibbs–Duhem equation (Blandamer et al., 2005b; Calderón et al., 2020c). Water activities can be retrieved from experimental measurements (osmotic coefficient, electric potential, etc.).

In this study, the water activity is calculated with the CMC based ionic surfactant activity (CISA) model (Calderón et al., 2020a) that accounts for changes in the micellization in aqueous surfactant solutions induced by the presence of an inorganic salt. The CISA model was constructed to describe the water activity and activity coefficients in ternary systems comprised of water, an ionic surfactant and an inorganic salt, both sharing a common ion (e.g. the sodium ion is the common ion shared by sodium decanoate and sodium chloride).

importance of considering the micellization can be noticed in Figure 9 that compares the variation of water activity in aqueous solutions with increasing surfactant concentration calculated with (left panel) and without micelle formation (right panel). Calculated values considering the existence of micelles as a component of the solution when surfactant concentration exceeds CMC, correspond to the experimental values way better than the ones calculated without it. This behavior repeats in ternary solutions of water, NaDec and NaCl. In the presence of NaCl, there is also a

significant effect of the inorganic salt concentration in the CMC. Figure 10 shows the variation of water activity in aqueous NaDec-NaCl solutions at different ratios of the solutes. We can observe how with increasing NaCl content, the CMC decreases indicating that micellization occurs at surfactant concentrations that are much lower than the ones required for micelle formation in pure water at the same temperature. It is common practice in calculations with the classical Köhler model to calculate the water activity at total droplet composition, and typically disregarding the possible existence of micelles in the droplet solution. Figures 9 and 10 indicate how this introduces a source of uncertainty in calculations of droplet growth along the Köhler curve.

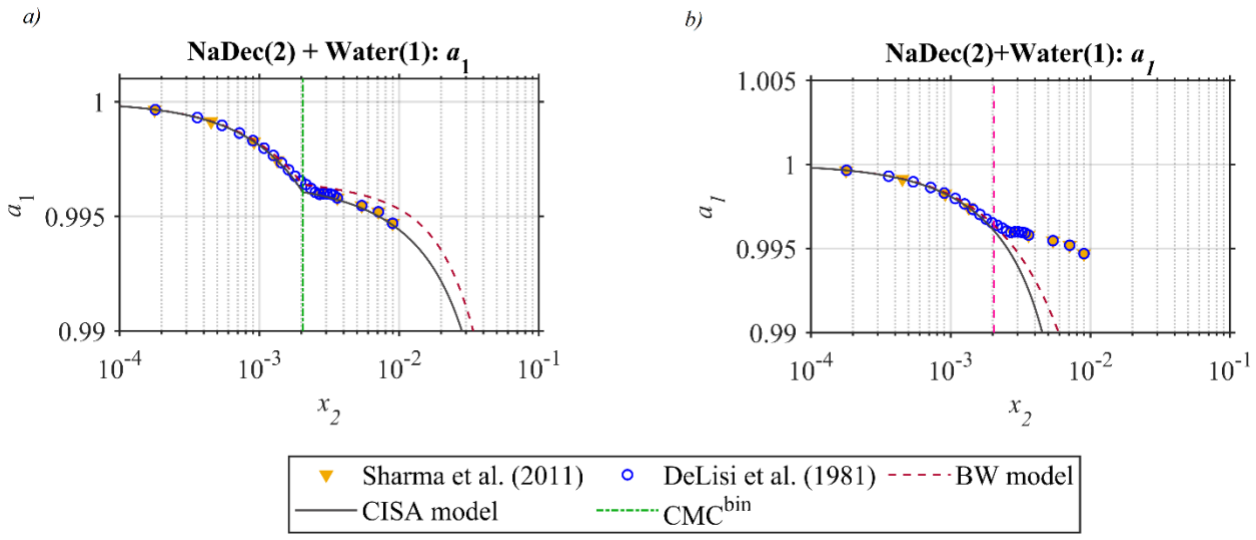

Figure 9 Water activity in aqueous solutions of sodium decanoate at 298 K calculated a) with micelle formation b) disregarding the micelle formation (Calderón et al., 2020b)

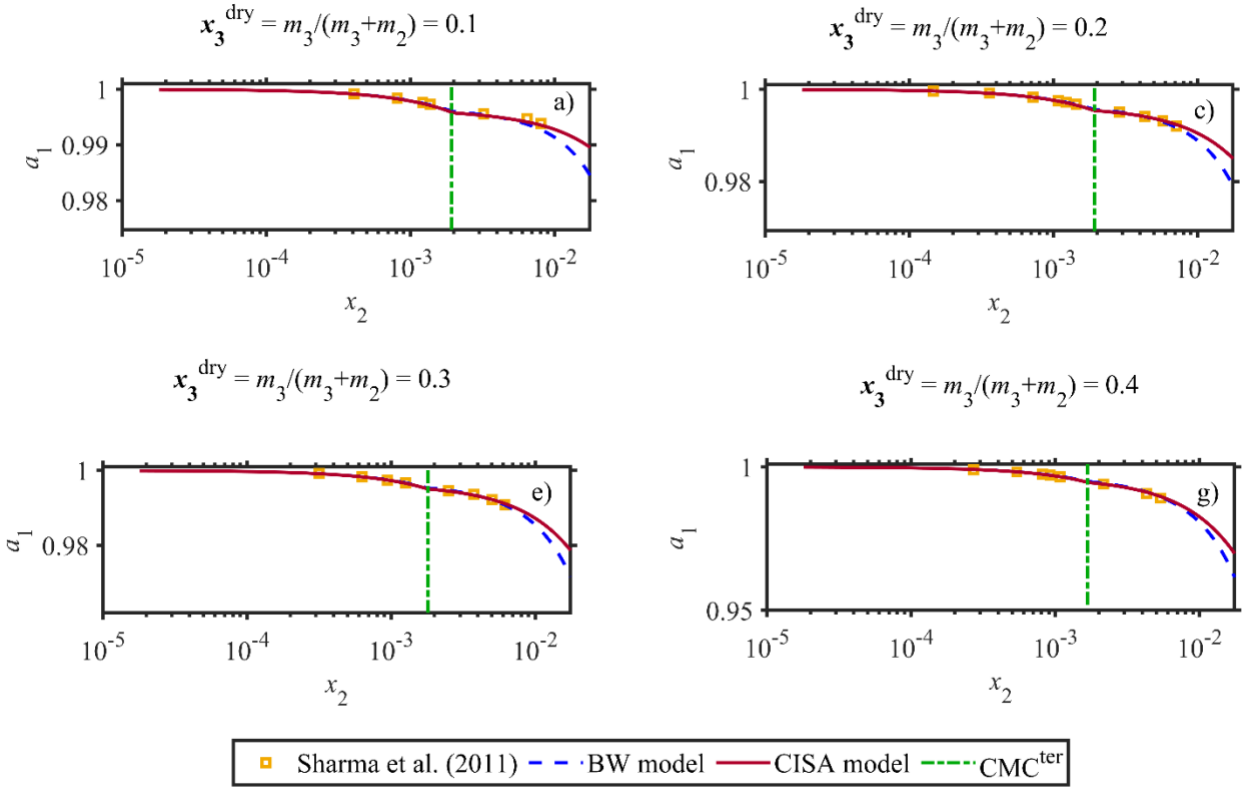

Figure 10 Variation of the water activity in aqueous solutions of sodium decanoate (2) and sodium chloride (3) at 298 K and different ratio of solutes in solution. The CMC is shown to highlight the variation in trends induced by micellization https://creativecommons.org/licenses/by/4.0/(Calderón et al., 2020b)

In terms of the surface tension, Figure 11 shows how with increasing concentrations of NaDec the surface tension of water is notably reduced up to a minimum reached at the CMC. This behavior is commonly represented with the Langmuir–Szyskowski equation

$\sigma = \sigma_w - a\ln(1 + m_2/b)$,

where σ_w is the surface tension of pure water at the correspondent temperature, *a* and *b* are constants determined by fitting of experimental data.

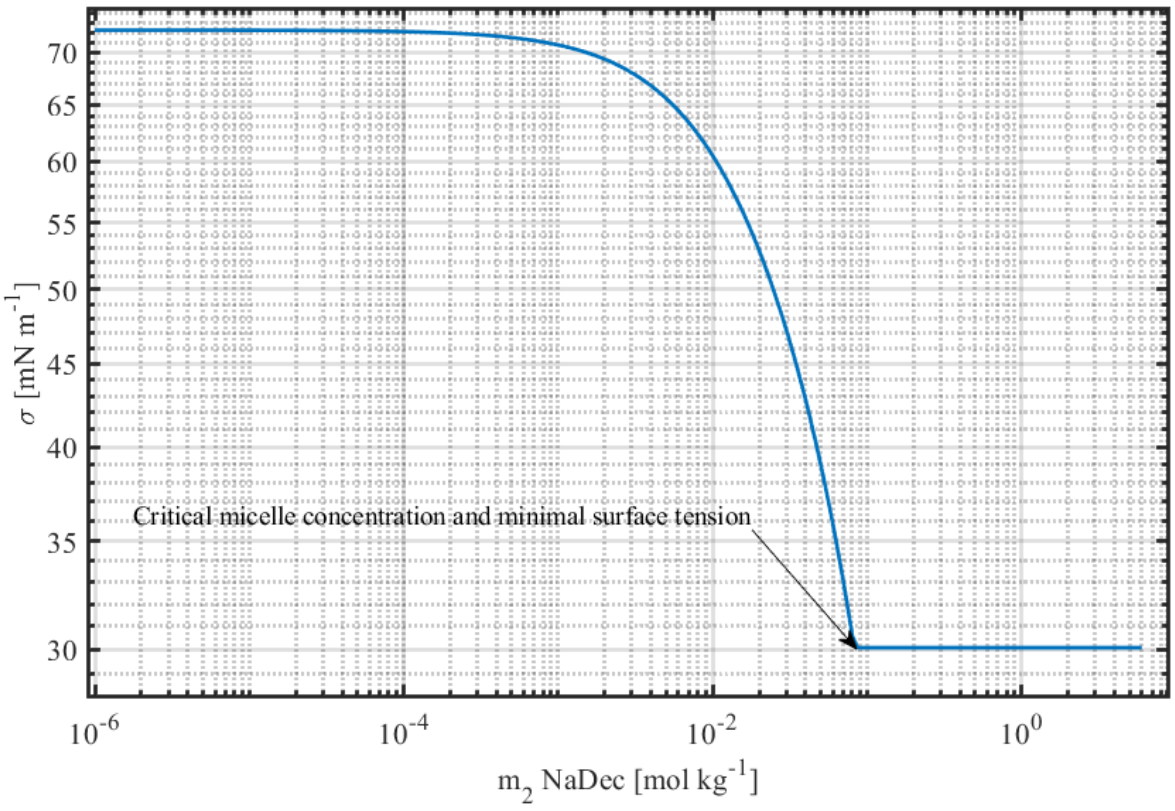

Figure 11 Variation of the surface tension of aqueous solutions of NaDec at 296 K as function of surfactant concentration https://creativecommons.org/licenses/by/3.0/ (Prisle et al., 2010)

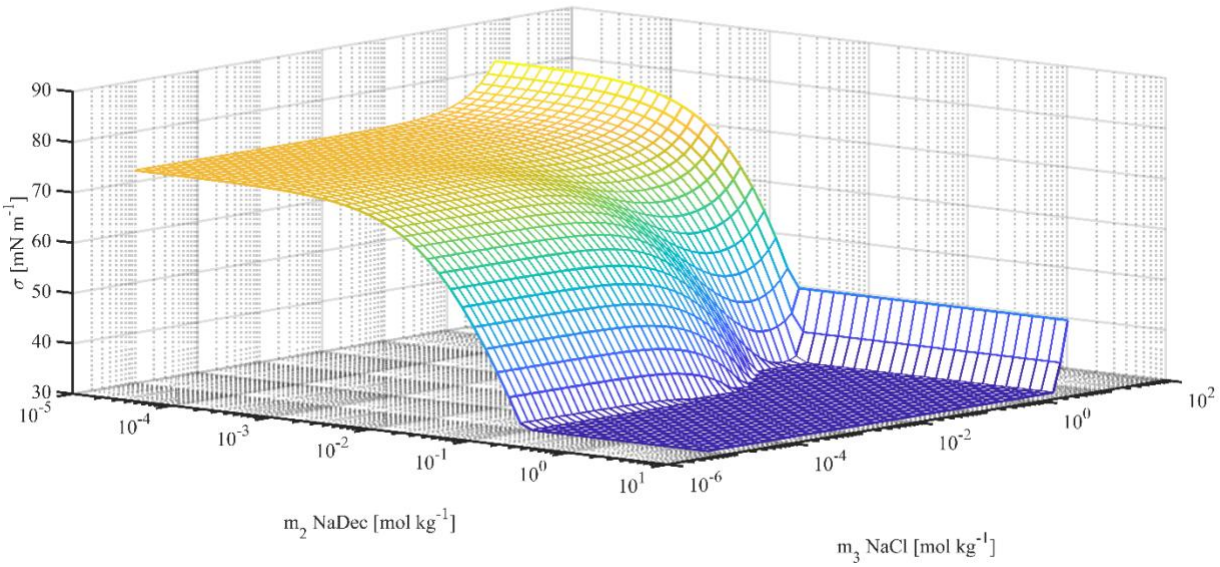

Figure 12 Variation of the surface tension of aqueous solutions of NaDec (2) and NaCl (3) at 296 K using the parametrization of Prisle et al. (2010) combined with the CMC-parametrization of Calderón et al. (2021) https://creativecommons.org/licenses/by/4.0/

When NaCl is added to the aqueous surfactant solution, the surface tension varies and a unit reduction in surface tension with increasing surfactant concentration is reached at a lower value as sodium ions enhance the adsorption of decanoate ions at the air-solution interface (Danov et al., 2014). The Langmuir–Szyskowski model is modified as follows (Prisle et al., 2010):

$$\sigma = \sigma_w + \left(\frac{d\sigma}{dm_3}\right) - a\ln(1 + m_2/b) \qquad \text{Eq. 6}$$

where the additional term $\left(\frac{d\sigma}{dm_3}\right)$ is equal to -1.61 mN (mol l^{-1})$^{-1}$ and the model parameters *a* and *b* become composition-dependent as follows:

$$a = a_1 + a_2 w_2 + a_3 w_2^2 \qquad \text{Eq. 7}$$
$$b = b_1 + b_2 w_2 + b_3 w_2^2$$

where w_2 represents the surfactant mass fraction in the dry particle solely composed of NaDec and NaCl.

Composition of aerosol particles

Aerosol particles are represented as spherical dry particles with radius R_p and a composition defined by the surfactant mass fraction

$$\epsilon_2 = \frac{w_2}{w_2 + w_3} \qquad \text{Eq. 8}$$

where w_2 and w_3 are the mass of surfactant and inorganic salt in a dry particle. The values of w_2 and w_3 in a dry particle of radius R_p relates to the total number of molecules per species n_2^T and n_3^T as

$$n_2^T = 0 \wedge n_3^T = \frac{4\pi}{3} R_p^3 \frac{\rho_3}{w_3}, for \epsilon_2 = 0 \qquad \text{Eq. 9}$$

and

$$n_2^t = \frac{\frac{4\pi}{3}R_p^3}{\frac{1}{\rho_2}+\frac{1}{\rho_3}\frac{(1-\epsilon_2)}{\epsilon_2}}\frac{1}{w_2} \wedge n_3^T = n_2\frac{w_2}{w_3}\frac{(1-\epsilon_2)}{\epsilon_2}, for \epsilon > 0, \qquad \text{Eq. 10}$$

where $i = 2{,}3$ refers to the properties of pure species, n_i^T is the total number of molecules, w_i is molecular mass and ρ_i is density species i in solid phase pure compound in solid phase.

Köhler calculations without bulk–surface partitioning using the classical Köhler model

The droplet growth was studied using the Köhler theory (Köhler, 1936) as a thermodynamic model that describes the equilibrium of water at the air-droplet interface in terms of the saturation ratio (S) and droplet radius R_d as

$$S \equiv \frac{p_1}{p_1^0} = a_1 exp\frac{2v_1\sigma^B}{RTR_d} \ . \qquad \text{Eq. 11}$$

Where p_1 is the equilibrium partial pressure of water over the solution droplet, p_1^0 is the saturation vapor pressure over a flat surface of pure water, a_1 is the activity of water, v_1 is the partial molar volume of water in the droplet solution, σ^B is the surface tension of the droplet bulk solution, R is the universal gas constant and T is the temperature. Each droplet is modelled as a sphere with a radius R_d. The total droplet composition is followed through the dilution of the initial number of solute molecules n_2 contained in a dry particle of radius R_p in droplets with sizes ranging between R_p and a droplet radius that it is well above the critical radius.

For each droplet size along the Köhler curve, the total droplet composition x^T in mole fraction is calculated resolving water from the droplet mass conservation in accordance with the modelling framework for bulk-surface partitioning as explained in the next section. This model is later identified as CK-model or classical Köhler model.

Köhler calculations without bulk-surface partitioning using the classical Köhler model

The Köhler model disregards effect of bulk–surface partitioning and depicts the droplet as a single compartment system. The model is a treatment for the droplet as a macroscopic solution. We can consider that the Köhler model (K) is as a partitioning model with null depletion rate for all components in the droplet solution and a droplet surface compartment of zero volume. In the Köhler model, the water saturation ratio is calculated assuming that the water activity of the droplet solution at total droplet composition $x^T = n^T / \sum n_i^T$ is given by the model of (Calderón et al., 2020c) and the surface tension of the droplet solution corresponds to that of pure water. The surface tension of the pure water is calculated with the model of Pátek et al. (2009).

For each droplet size expressed as droplet radius R_d we resolve the water mass from the droplet mass conservation equation

$$\frac{4\pi}{3} R_d^3 \rho(x^T) - n \cdot w = 0, \qquad \text{Eq. 12}$$

following the approach of (Malila & Prisle, 2018), where $\rho(x^T)$ is the density at the total droplet composition x^T and temperature T, w and n are vectors containing the molecular mass and the number of molecules of pure water and pure surfactant. The mathematical symbol $\cdot$ is the dot product between vectors.

Results of the K-model can be compared to those from the classical Köhler model to gain insight on the water activity effect, since the K-model includes solution nonidealities induced by interactions between ions after dissociation of the ionic surfactant and the inorganic salt, as well as those caused by the surfactant aggregation.

Köhler calculations with bulk-surface partitioning calculated with the monolayer model

The monolayer model (ML) calculates bulk depletion rates of all droplet constituents with droplet size and total composition dependencies. The droplet is represented as a closed system of two compartments, an inner or droplet bulk compartment of volume V^B and an exterior or droplet surface compartment of volume V^S with a spherical shell of thickness δ. The total number of molecules n^T

in a droplet of known size and composition is split between surface and bulk as n^S and n^B, respectively. The surface thickness δ is considered to be equivalent to the diameter of a spherical molecule which volume equates to the composition-weighted average molecular volume at surface condition as

$$\delta = \left(\frac{6}{\pi} x^S \cdot v\right)^{\frac{1}{3}} \qquad \text{Eq. 13}$$

where x^S is the vector containing the composition of the droplet surface compartment in molar fractions and $x^S \cdot v$ is the vector containing the molecular volume of pure compounds. Surface thickness cannot be wider than the diameter of a spherical molecule holding the largest molecular volume nor shorter than the diameter of a spherical molecule with the lowest volume per molecule as it is depicted in Figure 13. Limiting values of surface thickness are shown in Table 1.

The monolayer model must resolve the surface composition x^S under the constraint of droplet mass conservation until δ yields a surface composition x^S under the constraint of droplet mass conservation until δ yields a surface tension of the bulk solution equal to the surface volume fraction weighted average of pure component surface tension as

$$\sigma(x^B) = \phi^S \cdot \sigma = \sum_i \frac{v_i x_i^S}{x^S \cdot v} \sigma_i, \qquad \text{Eq. 14}$$

where $\sigma(x^B)$ is the surface tension of the droplet bulk solution, ϕ^S is the vector containing the volume fraction of all compounds in the droplet solution at surface composition x^S, while σ is the vector containing the surface tension for pure compounds.

The mass conservation for the droplet is represented as

$$x^T \frac{4}{3}\pi R_d^3 \frac{\rho(x^T)}{x^T \cdot M} = x^B \frac{4}{3}\pi (R_d - \sigma)^3 \frac{\rho(x^B)}{x^B \cdot M} + x^S \frac{4}{3}\pi (R_d^3 - (R_d - \delta)^3) \frac{\rho(x^S)}{x^S \cdot M} \qquad \text{Eq. 15}$$

x^T, x^B and x^S are vectors representing the composition of total droplet, droplet bulk and droplet surface solutions, respectively. $\rho(x^T), \rho(x^B)$ and $\rho(x^S)$ are the densities of the total droplet, droplet bulk solution and the droplet surface solution, M is the vector with the molecular weight of the pure compounds, σ_i and v_i represent the surface tension and molecular volume of species i as pure liquids. And where $x^b = \left(x_1^b, x_2^b, \ldots\right)$ are the bulk mole fractions $n_i^b / \sum_j n_j^b$ of each species i, v_i

and σ_i are the molecular volumes and surface tensions of each pure component i and the x_i^s are the surface mole fractions.

Here, the surface tension will be calculated using the pseudo-binary approximation of Malila & Prisle (2018), giving the surface tension as

$$\sigma\left(x_{13}^b, x_2^b\right) = \frac{\sigma_{13} v_{13} x_{13}^s + \sigma_2 v_2 x_2^s}{v_{13} x_{13}^s + v_3 x_3^s}, \qquad \text{Eq. 16}$$

where the subscript 1 refers to water, 2 to the surfactant and 3 to the inorganic salt.

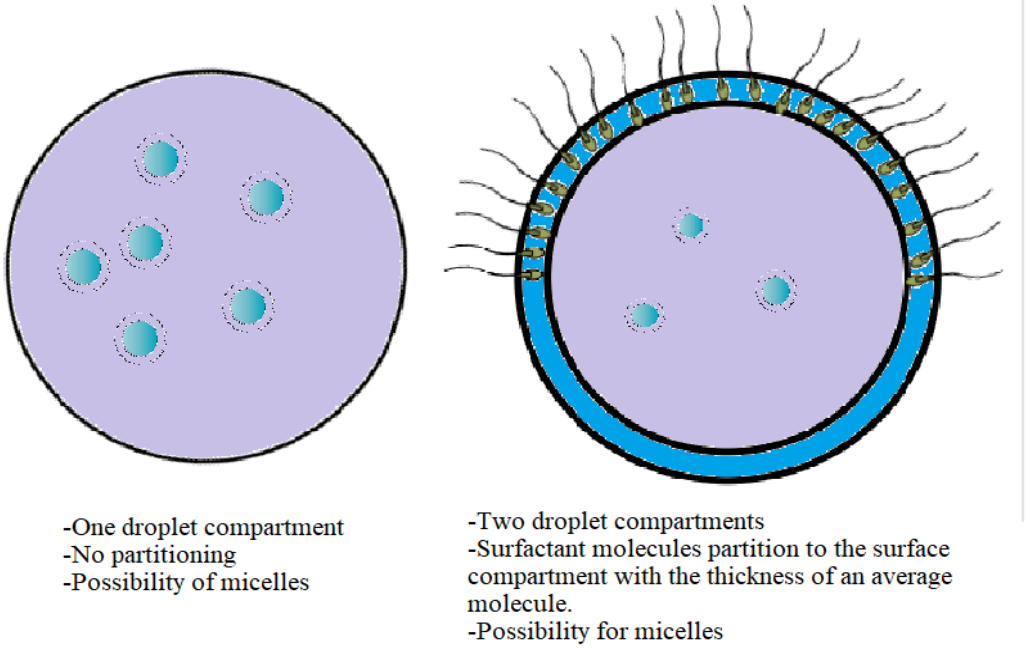

Figure 13 Schematic description of the fundamental assumptions in the monolayer model with respect to the droplet structure.

Results

Aerosol composition effect on droplet activation

We calculated the Köhler curve and activation point of a 15 nm dry particle with surfactant mass fractions of 0.25, 0.50, 0.75 and 0.95. Keeping the same size of the dry particle, we can study separately the effect of the aerosol composition in the variation of the activation point. The selected particle size corresponds to the lower limit of the dominate mode in the volume size distribution of secondary marine aerosols observed in a controlled ocean system study by Mayer et al. (2020). The findings said that under the course of a phytoplankton bloom with natural atmospheric conditions, the secondary marine aerosols (SMA) are the ones controlling marine cloud properties. SMA are generated by the oxidation of biogenic sulfur-containing gases such as dimethyl sulfide released by phytoplankton. Figure 14 shows the correlation of SMA total volume and chlorophyl concentrations. Chlorophyl is produced by phytoplankton and serves as a marker for biological activity in the oceans. Figure 14 also shows that SMA aerosols particles are on the submicron range with a dominant mode between 15 nm and 30 nm in radius.

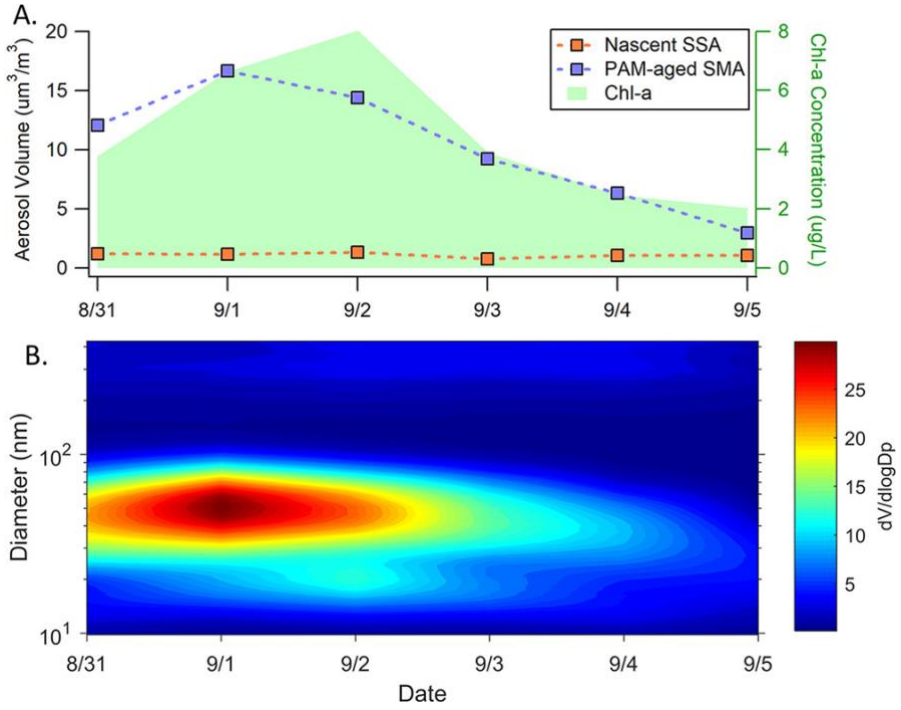

Figure 14 Daily average of aerosol volume concentration and volume size distribution of aerosol particles collected from an isolated system marine aerosol reference tank (MART) during a phytoplankton bloom A) Total aerosol volume concentration vs. Chlorophyl-a (Chl-a) concentration in an oxidative flow reactor (OFR), Nascent SSA stands for Primary Sea Spray Aerosols, PAM-aged SMA stands for Secondary Marine Aerosol. B) Aerosol volume size distribution. (https://pubs.acs.org/doi/10.1021/acscentsci.0c00793 Further permissions related to the material excerpted should be directed to ACS. (Mayer et al., 2020a)

In Figure 15 we show Köhler curves calculated with the K-model and the ML-model for different aerosol compositions. Conditions at the activation point are summarized in Table 2. The critical supersaturation calculated with the Köhler model ranges from 1% to 2.7% with a dry particle of 15 nm. This indicates these kinds of droplets have little to no possibility of activation under natural conditions. The sea spray aerosols contribution to the CCN population is less than 30% in normal marine boundary layer conditions where the supersaturation range is from 0.1% to 1% (Quinn et al., 2017). The one percent supersaturation needed for activation is unlikely, but possible in the nature. Typical stratocumulus clouds have supersaturation of 0.2% and large cumulus clouds 0.5%. The 1 – 2% supersaturation is achieved in circumstances where there is strong convection in the cloud (Devenish et al., 2016). The monolayer model predicts a much lower needed supersaturation in for the droplet range. The critical radius predicted with the Monolayer model is larger than the critical radius calculated with the Köhler model. While increasing the mass fraction of surfactant, the difference increases in the critical radius predicted. The Köhler model predicts more extreme decrease in the critical radius. The monolayer model gives conditions for activation that are 60 – 80% of those predicted by the Köhler model mostly due to the reduction of the surface tension. Noteworthy is that

the difference of the critical conditions the models predict is almost negligible with close to 0 mass fraction of the surfactant as expected.

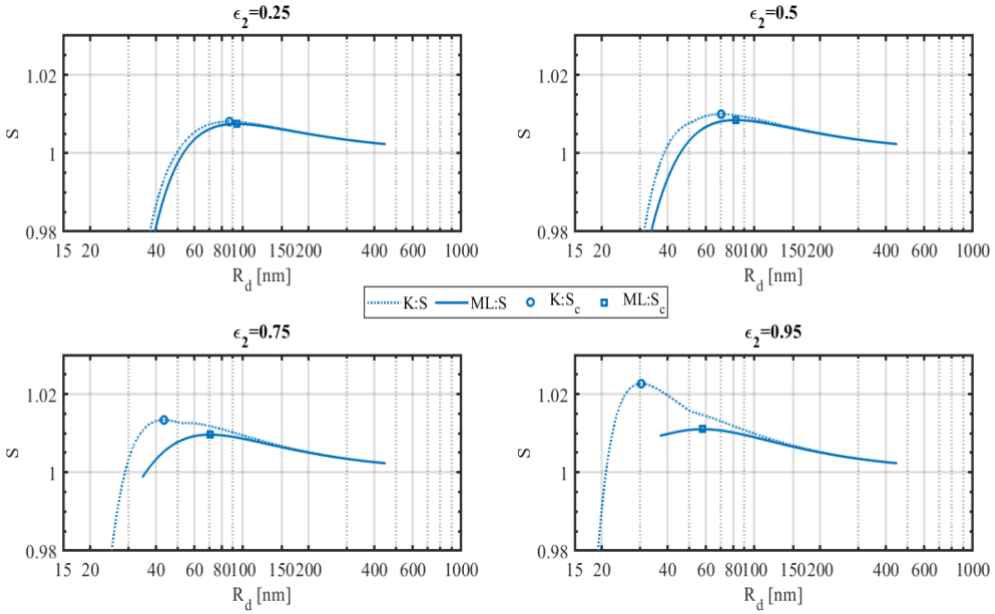

Figure 15 Köhler curves for a dry particle of 15 nm in radius 15 nm radius containing different mass ratios of NaDec(2) and NaCl(3) calculated with the K-model and the ML-model. Critical points are marked in each case.

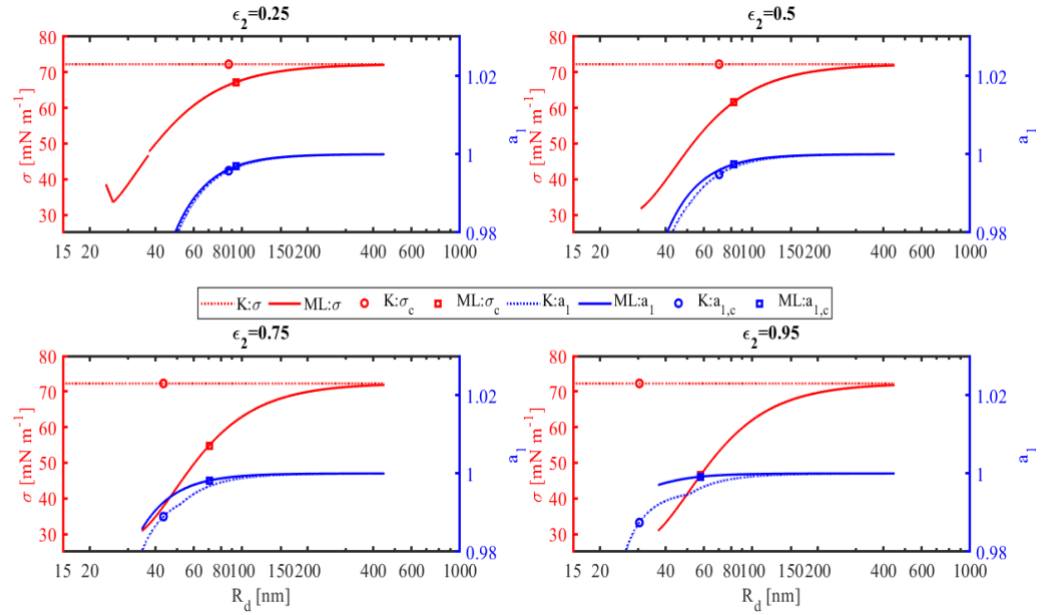

Figure 16 Variation of the surface tension (red) and water activity (blue) along the Köhler curves for a dry particles with 15 nm radius containing different mass ratios of NaDec(2) and NaCl(3). Critical points are marked in each case.

Figure 16 shows the variation of the surface tension and water activity of the droplet bulk solution along Köhler curves, together with the conditions at the critical point. At surfactant mass fractions below 0.5, there are no significant differences in the water activity calculated with both models. Differences in the ML-critical point, larger droplet size and higher saturation at activation, can be explained by the reduction in the droplet surface tension which can be as large as 44.4% relative to the value of pure water (i.e. the surface tension at droplet activation is 55.6% of the pure water surface tension). At higher surfactant mass fractions in the dry particle ($\varepsilon_2 \geq 0.75$) differences in water activity and surface tension accentuate. The K-model predicts that droplet activation occurs when the droplet bulk solution contains micelles, as the critical point is to the left of the inflection point caused by micellization. We can notice in the lower panels of Figure 16 that micellization induces a change in the variation of water activity during droplet growth. This change is then transfered to the Köhler curve. With lower water activity at increasing surfactant content in the dry particle, the Raoult effect compensates the Kelvin effect, and the droplet activation occurs with a lower growth factor at a higher critical supersaturation, compared to the ML-model.

For a single particle size, the addition of surfactant has the effect of lowering the surface tension. When the concentration exceeds the CMC the surface tension remains at a constant value regardless of the addition of the amount of surfactant. The K-model does not consider changes in surface tension, but instead assumes that the droplet surface tension stays close to that of pure water during droplet growth. This implicates the ML-model is a more realistic representation of a real droplet as the surface tension reduction is significant for a single droplet. The reason this is not implemented in models yet to a large extent is that these effects of surfactants had not been confirmed experimentally until the work of Bzdek et al. (2020).

For the same dry particle size, increasing surfactant mass fraction causes the activated droplets to be a smaller size, which requires a higher critical value of the supersaturation. The monolayer model gives conditions for activation that are 8% – 51% diminished of those predicted by the Köhler model mainly because of the reduction of the droplet solution surface tension at the critical point. Bulk-surface partitioning calculated with the monolayer model predicts activation with surface tension depression of 10% – 38% relative to the surface tension of pure water depending on the amount of surfactant.

Table 2 Conditions at the activation point for a dry particle composed by a 15 nm core of NaCl and coated with NaDec. Results from the K-model and ML-model.

Dry Particle radius (nm)	NaDec mass fraction	K-model*			ML-model			
		Critical radius (nm)	Critical supersaturation (%)	Water activity	Critical radius (nm)	Critical supersaturation (%)	Water activity	Surface tension (N m^{-2})
15	0.25	86.65	0.81	0.9958	93.58	0.75	0.997	0.0672
15	0.50	70.34	1.00	0.9949	82.10	0.85	0.997	0.0616
15	0.75	43.48	1.34	0.9890	70.54	0.96	0.998	0.0549
15	0.95	30.28	2.27	0.9875	57.71	1.10	0.999	0.0465

*The surface tension is modeled as the surface tension of pure water.

Figure 17 summarizes the variability in the critical saturation and the critical radius after changing the mass fraction of surfactant in a dry particle of 15 nm radius between pure NaCl and pure NaDec. Dotted lines show how both models predict an increase in critical saturation when the surfactant mass fraction is increased, increments of the ML-model are moderate compared to those predicted by the K-model. The K-model predicts the presence of micelles in the droplet solution at the activation point when the surfactant mass fraction is between 0.69 and 0.70. Micellization produces a drastic reduction in water activity that translates into larger critical saturation and smaller critical radius due to the dominance of the Raoult term.

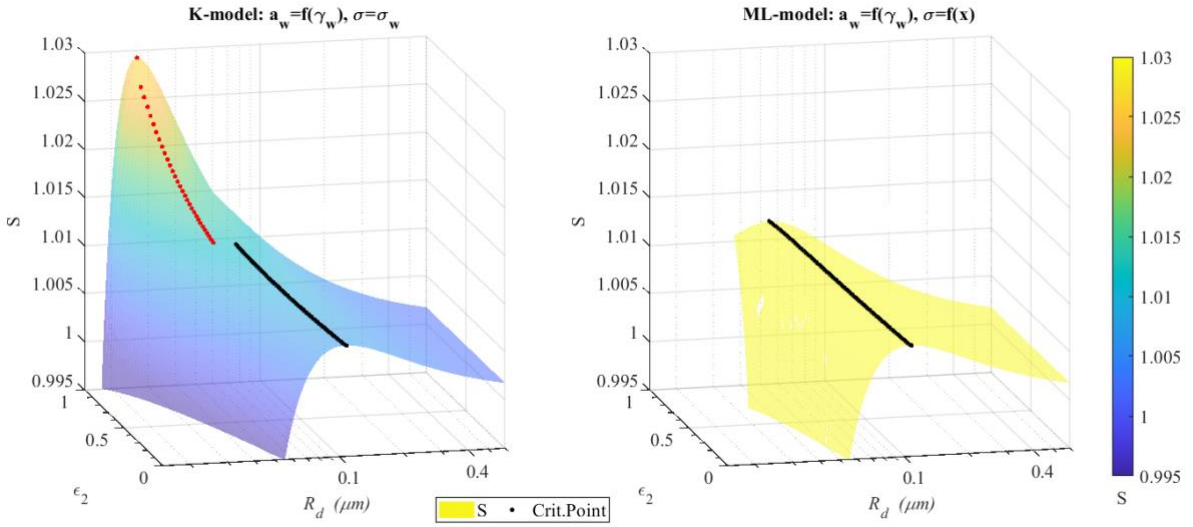

Figure 17 Composition-dependence of the critical point for a dry particle composed by NaDec and NaCl with 15 nm radius ($\varepsilon_2 = 0$ pure NaCl, $\varepsilon_2 = 1$ pure NaDec). If the critical point is designated with a red circle, it means that the droplet solution contains micelles.

Figure 15, Figure 16 and Figure 17 demonstrate that the modelling framework used to estimate the activation point of surfactant-enriched aerosols is very important as the critical diameter or droplet size at activation can vary between models. The critical diameter is often used as an input variable in parameterizations of cloud droplet formation (Morales Betancourt & Nenes, 2014).

The particle size has a strong influence on the aerosol water uptake. It defines the surface available for collision and condensation of water molecules and controls the Kelvin effect through the curvature of the air-droplet interface. For this reason, we studied previously the effect of particle composition keeping the same particle size without any consideration of particle morphology. However, in the atmosphere, the particle morphology varies depending on its formation mechanism, aging time and reaction history. Some morphologies observed in single-particle analysis are homogeneous-like structures such as core-shell and dumbbell structure; while others comprise one phase irregularly dispersed in other (Li et al., 2016; Liu et al., 2017). The core-shell structure has been recently identified as one of the most common morphologies in single-particle analysis of submicron marine particles during a phytoplankton bloom (Kaluarachchi et al., 2022a).

We explored the variation in the Köhler curve and activation point of a 15 nm-radius dry particle composed of pure NaCl when it is coated with a NaDec layer of different thickness going from 1 nm to 10 nm. In this case, both, particle size and composition are changing simultaneously simulating particle formation at different degrees of organic enrichment of the sea surface microlayer. It is known that sub micrometer sea spray aerosols (SSAs) are mainly formed by film drops produced from bursting bubble-cap films, which become enriched with hydrophobic organic species contained within the sea surface microlayer (Wang et al., 2017).

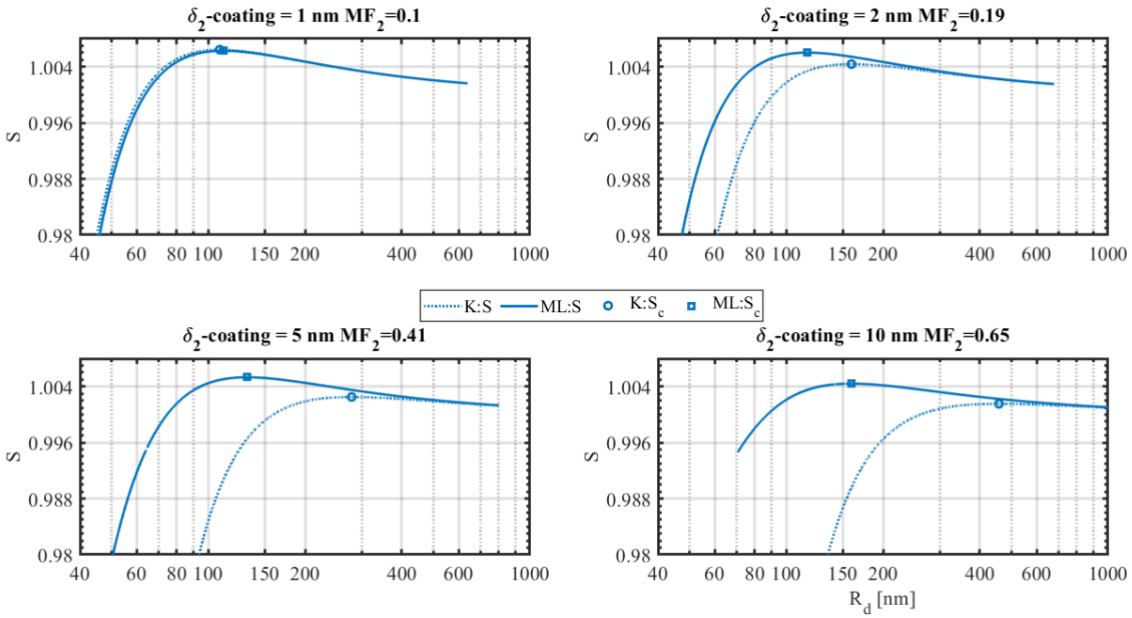

Figure 18 Köhler curves for dry particles composed of an inorganic NaCl core of 15 nm-radius coated with a NaDec layer of different thickness (δ_2). Critical points are marked in each case.

By visual inspection of Figure 18 and Figure 19 we can see the effect of increasing the coating of organic matter versus increasing the mass fraction of organic matter in a 15 nm particle. For the same number of NaCl molecules in the dry particle, increasing thickness of the surfactant coating and therefore increasing effective particle size, produce activating droplets with increasing critical diameter varying between 108.7 nm and 458.3 nm and critical supersaturation between 0.64% and 0.15%. Conditions at the critical point for each coating condition are summarized in Table 3.

Table 3 Conditions at the activation point for a dry particle composed by a 15 nm core of NaCl and coated with NaDec. Results from the K-model and ML-model.

Coating thickness (nm)	Dry particle radius (Seed + Coating)	K-model*			ML-model			
		Critical radius (nm)	Critical supersaturation (%)	Water activity	Critical radius (nm)	Critical supersaturation (%)	Water activity	Surface tension (N m^{-2})
1	16	108.7	0.644	0.997	111.4	0.628	0.997	0.071
2	17	159.6	0.438	0.998	116.3	0.602	0.997	0.069
5	20	279.2	0.251	0.999	132.0	0.532	0.998	0.065
10	25	458.3	0.153	0.999	159.5	0.441	0.999	0.061

*The surface tension is modeled as the surface tension of pure water.

Both models predict larger sizes for activating droplets when the coating thickness increases, but droplet enlargement is more pronounced by the K-model.

The mesocosm experiment studies for chlorophyll-a during phytoplankton blooms show that there is an increase in the amount of organic matter suspended in air during the bloom (Kaluarachchi et al., 2022b). The chlorophyll-a i.e. phytoplankton biomass correlates with secondary marine aerosols made of sulfate, ammonium and organics (Mayer et al., 2020a). The secondary marine aerosols are the primary source of surfactants in marine environments (Mayer et al., 2020a). Thus during these episodes of biological activity, it is likely that there are more particles that activate with a lower threshold to CCN in the sea surface layer. The possible outcome of this is a more robust cloud albedo depending on the refractive properties of the biological material. The fact that leads to this is if more particles are suspended in air and are available for the water intake from the atmosphere, the particles never achieve CCN status. During times when sufficient water is available the cloud becomes denser, and the possibility of precipitation increases. In wintertime in the Arctic the cloud-aerosol interactions are even more pronounced due to the decrease in solar radiation in the wintertime. There is a contribution to warming as increased cloud albedo can keep an increased amount of longwave radiation close to the surface (Kirpes et al., 2019).

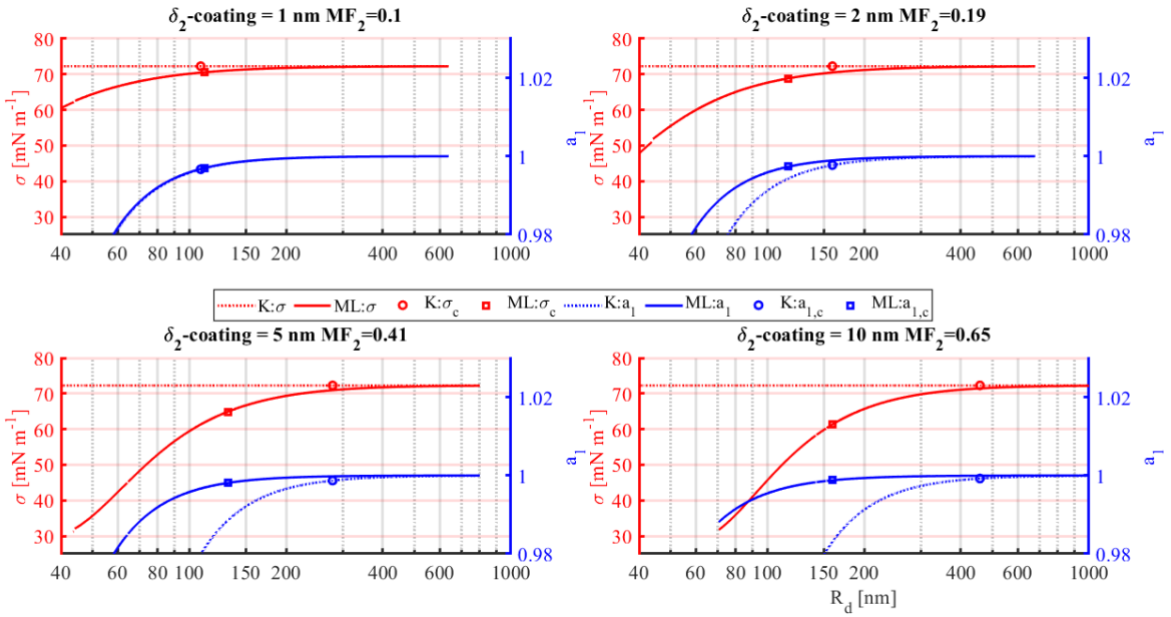

Figure 19 Variation of the surface tension (red) and water activity (blue) along the Köhler curves for a dry particle composed of an inorganic NaCl core of 15 nm-radius coated with NaDec layers of different thickness (δ_2). Critical points are marked in each case.

Growth factor maps for NaDec/NaCl aerosol particles

Panels of Figure 20 summarizes the variability in growth factor at the critical point (GFc) and critical supersaturation of particles with dry size ranging from to 24 nm and 500 nm with composition ranging from pure NaCl to pure NaDec. The growth factor is defined as the ratio between the dry particle size and droplet size at the critical point. ML-model outputs are plotted as contour plot while CK-model and K-model outputs are plotted as dashed lines. The critical supersaturation in the left panel and the growth factor at the critical point can be read using the x-coordinate as the dry particle diameter and the y-coordinate as the dry particle composition (i.e. mass fraction of sodium decanoate).

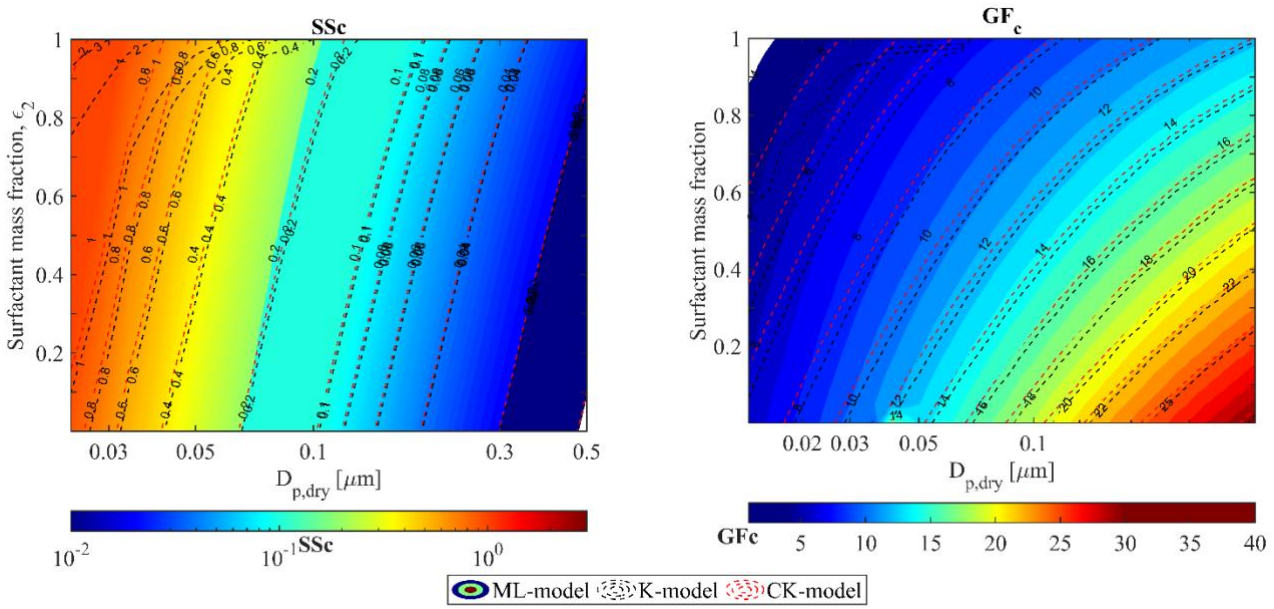

Figure 20 Critical point calculated with the CK-model, K-model, and ML-model for dry particles composed of NaCl and NaDec. Left panel: critical supersaturation, right panel: growth factor. Black dashed lines correspond to the K-model, red dashed lines correspond to the CK-model.

The surfactant induced effects start significantly affecting the modeling of the droplets when the dry particles are below 100 nm and the surfactant mass fraction is over 0.4 - 0.5. We can deduce the same from the Figure 20 that the consideration of bulk surface partitioning is important below 100 nm and the effect increases significantly after the mass fraction of organics surpasses 0.4. The reduction of surface tension below 90% of the value of pure water is possible for all particles below 300 nm as seen in Figure 21. Also, the thickness of the monolayer has a correlation to this behavior.

In Kirpes et al. (2019) they found the median volume fraction in SSA-organic enriched aerosols was 0.45. In our study the 0.4 mass fraction correlates to a surfactant volume fraction of 0.54. It is reasonable to say that the presence of organics in a particle has a significant chance to have consequential effect on the properties of the particle. We have shown that disregarding some or most

of the surfactant effects through the classical Köhler and the K-model would lead to wrong predictions of the critical point, in both, size and critical supersaturation. This means that if a model uses the critical supersaturation (e.g. SSair_parcel >= SSc), or the critical size (e.g. Dwet > Dc) as a criteria for particle activation, these would lead to wrong estimates to CCN concentrations.

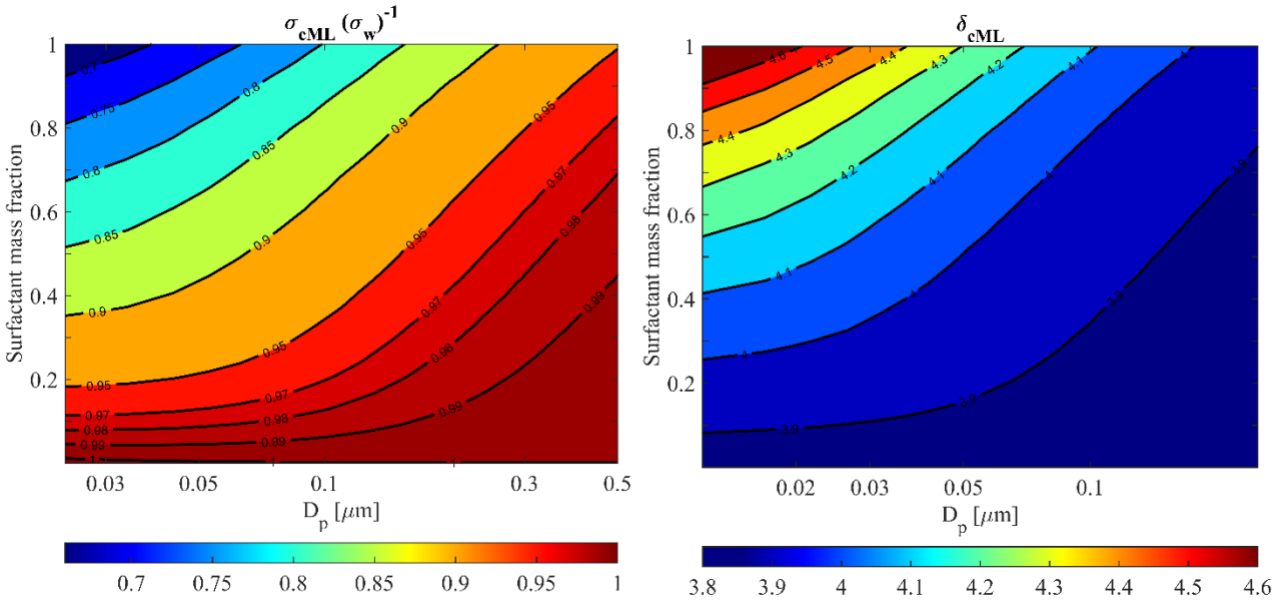

Figure 21 Droplet solution properties at the activation point calculated with the Monolayer model for dry particles composed of NaCl and NaDec.. Left panel: Surface tension depression at the activation point calculated as a fraction of the surface tension of pure water Right panel: Thickness of the monolayer in angstroms

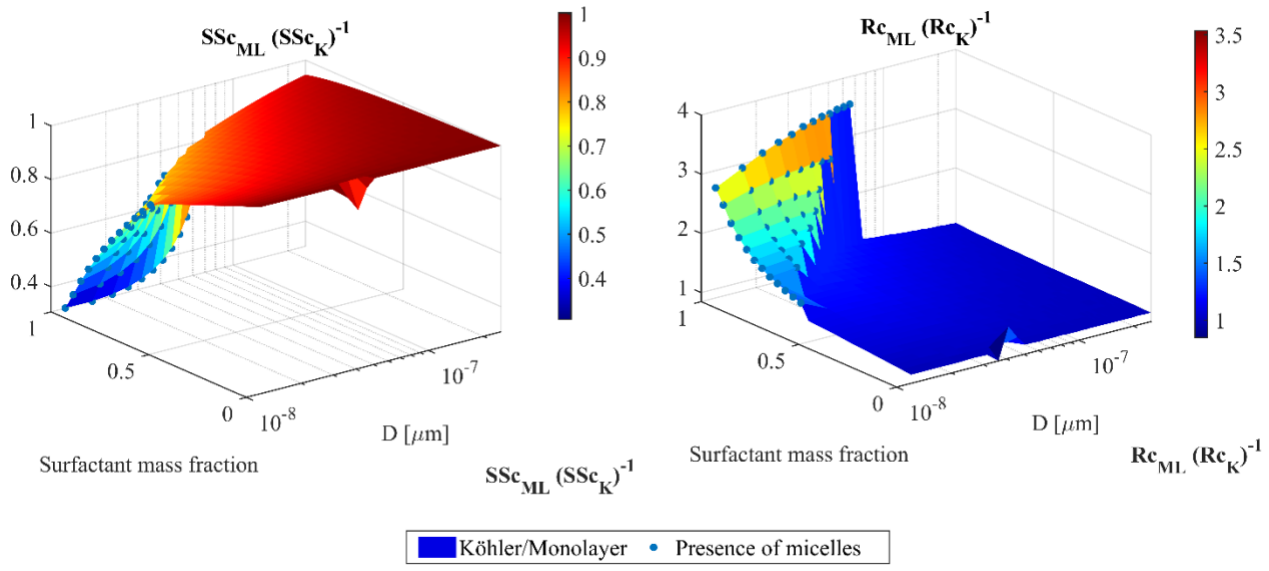

Figure 22 a) Surfactant-induced effects on the critical point of sodium decanoate and sodium chloride mixed particles considering bulk–surface partitioning with the monolayer model. b) Surfactant-induced effects on the critical radius of sodium decanoate and sodium chloride mixed particles considering bulk–surface partitioning with the monolayer model.

Increasing surfactant mass fractions lead to larger critical supersaturations (SSc) seen on Figure 20. However, the ML-model gives lower values than the K-model (Figure 22) due to the combined effect on bulk–surface partitioning and surface tension depression (Figure 21). The Figure 22 shows that the supersaturation needed for droplet activation decreases towards bigger dry particles. The graph shows the calculation of the CK - model, K-model and the monolayer model. The comparison of the three models show that the monolayer model predicts the critical supersaturation to be lower than those calculated with the other two. The result agrees with the study of Prisle et al., (2008) where it was found that the modeling, where bulk-surface partitioning was not included, underpredicted the critical supersaturation values, whereas the results were in better agreement with the calculation values when partitioning was included. The interesting notification of the plots is the increasing surfactant fraction lowering the surface tension. When decreasing the dry particle size, the change in the critical supersaturation differences becomes larger. The result indicates the importance of partitioning in modeling cloud activation properties of droplets.

There are signs in literature that surfactants enhance the activation of larger droplets (Sorjamaa et al., 2004). In Figure 22 b) is seen the critical radii comparison of a droplet plotted against the dry particle diameter and surfactant mass fraction. The monolayer model predicts the critical droplet size to be larger throughout the lower range of particles (the relevant size range for marine aerosol count during the phytoplankton bloom (Mayer et al., 2020b)) and surfactant mass

fraction spectrum $(0.25 - 0.95)$ seen here.

Conclusions

Aggregation process of surfactants called micellization is a complex thermodynamic problem which depends on the concentration of also other species in the solution. The monolayer model uses a composition dependent function successfully to represent an experimentally feasible way to overcome limitation set by a lack or scarcity of activity coefficient data (Calderón et al., 2020c).

For the K-model, water activities show the presence of micelles in a significant part of the particle size-composition range. This suggests that current estimations of the cloud forming potential of secondary marine aerosols with the conventional setting of the Köhler model could be misled by using the corrected water mole fraction as a measure of the water activity. More precise and computationally efficient ways of property calculation are needed to understand the role of biogenic aerosols in the radiative forcing of marine clouds.

The monolayer model showed that it could be physically possible for the smallest dry particle range around 15 nm to activate in atmospheric conditions. That would mean increased droplet number concentration in clouds which would increase cloud albedo. The critical supersaturation calculated with the Köhler model implies that the current modeling neglects the smallest dry particle range to be able to activate. In atmospheric conditions air supersaturation is generally around $0.1\% - 0.4\%$ but can achieve as high values as 1% in clean conditions (Kroflič et al., 2018; Quinn et al., 2015). The study by Quinn et al. (2015) says the critical radius of particles values vary between 20 nm – 150 nm on normal conditions but activated droplets can be as small as 10 nm – 15 nm in radius. Our calculations agree with these results as both models predict the minimum critical particle radius to be around 20 nm – 70 nm. The monolayer model prediction is a bit more restrictive compared to the Köhler model result. The ML-model predicts a smaller need of supersaturation for droplets to activate, when going toward the 10 nm point in radius the needed supersaturation closes to $0.8\% - 1\%$ increasing with increasing surfactant fraction. In atmospheric conditions a small particle with close to 95% surfactant mass fraction in conditions with that high supersaturation is rare. For a limiting droplet size defined by the supersaturation in the air parcel, the larger critical droplet size predicted with the monolayer model results in a larger droplet number concentration in clouds compared to the Köhler model. The more particles there are taking up water in the cloud the less likely it gets for an individual droplet to become a CCN, this would result in a decrease in

precipitation. Taken from real atmospheric conditions it is possible for a single particle in this range to activate, but in average conditions it is more likely that there is a range of particles under 20 nm in radius left inactivated. The new composition-dependent parametrizations of water activity and density including micelles show a different perspective of the activation efficiency of surfactant-enriched aerosols. Even when these are surrogates of primary marine aerosols (enriched in NaCl not in SO_4 as the secondary marine aerosols), the interaction organic/inorganic controlling the surfactant behavior are very similar.

References

Abd El-Lateef, H. M., Tantawy, A. H., & Abdelhamid, A. A. (2017). Novel Quaternary Ammonium-Based Cationic Surfactants: Synthesis, Surface Activity and Evaluation as Corrosion Inhibitors for C1018 Carbon Steel in Acidic Chloride Solution. *Journal of Surfactants and Detergents*, *20*(3), 735–753. https://doi.org/https://doi.org/10.1007/s11743-017-1947-7

Abdul-Razzak, H., & Ghan, S. J. (2000). A parameterization of aerosol activation: 2. Multiple aerosol types. *Journal of Geophysical Research: Atmospheres*, *105*(D5), 6837–6844. https://doi.org/10.1029/1999JD901161

Abdul-Razzak, H., & Ghan, S. J. (2004). Parameterization of the influence of organic surfactants on aerosol activation. *Journal of Geophysical Research: Atmospheres*, *109*(3), 1–11. https://doi.org/10.1029/2003jd004043

Alpert, P. A., Ciuraru, R., Rossignol, S., Passananti, M., Tinel, L., Perrier, S., Dupart, Y., Steimer, S. S., Ammann, M., Donaldson, D. J., & George, C. (2017). Fatty Acid Surfactant Photochemistry Results in New Particle Formation. *Scientific Reports*, *7*(1), 12693. https://doi.org/10.1038/s41598-017-12601-2

Asa-Awuku, A., Sullivan, A. P., Hennigan, C. J., Weber, R. J., & Nenes, A. (2008). Investigation of molar volume and surfactant characteristics of water-soluble organic compounds in biomass burning aerosol. *Atmospheric Chemistry and Physics*, *8*(4), 799–812. https://doi.org/10.5194/acp-8-799-2008

Blandamer, M. J., Engberts, J. B. F. N., Gleeson, P. T., & Reis, J. C. R. (2005a). Activity of water in aqueous systems; A frequently neglected property. *Chemical Society Reviews*, *34*(5), 440–458. https://doi.org/10.1039/b400473f

Blandamer, M. J., Engberts, J. B. F. N., Gleeson, P. T., & Reis, J. C. R. (2005b). Activity of water in aqueous systems; A frequently neglected property. *Chemical Society Reviews*, *34*(5), 440–458. https://doi.org/10.1039/b400473f

Burdette, T. C., & Frossard, A. A. (2021). Characterization of seawater and aerosol particle surfactants using solid phase extraction and mass spectrometry. *Journal of Environmental Sciences*, *108*, 164–174. https://doi.org/https://doi.org/10.1016/j.jes.2021.01.026

Burrows, S. M., Butler, T., Jöckel, P., Tost, H., Kerkweg, A., Pöschl, U., & Lawrence, M. G. (2009a). Bacteria in the global atmosphere – Part 2: Modeling of emissions and transport between different ecosystems. *Atmospheric Chemistry and Physics*, *9*(23), 9281–9297. https://doi.org/10.5194/acp-9-9281-2009

Bzdek, B. R., Reid, J. P., Malila, J., & Prisle, N. L. (2020). The surface tension of surfactant-containing, finite volume droplets. *Proceedings of the National Academy of Sciences of the United States of America*, *117*(15), 8335–8343. https://doi.org/10.1073/pnas.1915660117

Calderón, S. M., Malila, J., & Prisle, N. L. (2020a). Model for estimating activity coefficients in binary and ternary ionic surfactant solutions. *Journal of Atmospheric Chemistry*, *77*(4), 141–168. https://doi.org/10.1007/s10874-020-09407-4

Calderón, S. M., & Prisle, N. L. (2021). Composition dependent density of ternary aqueous solutions of ionic surfactants and salts: Capturing the effect of surfactant micellization in atmospheric droplet model solutions. *Journal of Atmospheric Chemistry*. https://doi.org/10.1007/s10874-020-09411-8

Chang, D. Y., Lelieveld, J., Tost, H., Steil, B., Pozzer, A., & Yoon, J. (2017). Aerosol physicochemical effects on CCN activation simulated with the chemistry-climate model EMAC. *Atmospheric Environment*, *162*, 127–140. https://doi.org/10.1016/J.ATMOSENV.2017.03.036

Clint, J. H. (1992). Nature of surfactants. In *Surfactant Aggregation* (pp. 1–12). Springer, Dordrecht. https://doi.org/10.1007/978-94-011-2272-6_1

Cochran, R. E., Laskina, O., Trueblood, J. V., Estillore, A. D., Morris, H. S., Jayarathne, T., Sultana, C. M., Lee, C., Lin, P., Laskin, J., Laskin, A., Dowling, J. A., Qin, Z., Cappa, C. D., Bertram, T. H., Tivanski, A. V., Stone, E. A., Prather, K. A., & Grassian, V. H. (2017). Molecular Diversity of Sea Spray Aerosol Particles: Impact of Ocean Biology on Particle Composition and Hygroscopicity. *Chem*, *2*(5), 655–667. https://doi.org/10.1016/j.chempr.2017.03.007

Danov, K. D., Kralchevsky, P. A., & Ananthapadmanabhan, K. P. (2014). Micelle–monomer equilibria in solutions of ionic surfactants and in ionic–nonionic mixtures: A generalized phase separation model. *Advances in Colloid and Interface Science*, *206*, 17–45. https://doi.org/10.1016/J.CIS.2013.02.001

De Leeuw, G., Andreas, E. L., Anguelova, M. D., Fairall, C. W., Lewis, E. R., O'Dowd, C., Schulz, M., & Schwartz, S. E. (2011). Production flux of sea spray aerosol. *Reviews of Geophysics*, *49*(2), 1–39. https://doi.org/10.1029/2010RG000349

Delort, A.-M., Vaïtilingom, M., Amato, P., Sancelme, M., Parazols, M., Mailhot, G., Laj, P., & Deguillaume, L. (2010). A short overview of the microbial population in clouds: Potential roles in atmospheric chemistry and nucleation processes. *Atmospheric Research*, *98*(2), 249–260. https://doi.org/https://doi.org/10.1016/j.atmosres.2010.07.004

Després, VivianeR., Huffman, J. A., Burrows, S. M., Hoose, C., Safatov, AleksandrS., Buryak, G., Fröhlich-Nowoisky, J., Elbert, W., Andreae, MeinratO., Pöschl, U., & Jaenicke, R. (2012). Primary biological aerosol particles in the atmosphere: a review. *Tellus B: Chemical and Physical Meteorology*, *64*(1), 15598. https://doi.org/10.3402/tellusb.v64i0.15598

Devenish, B. J., Furtado, K., & Thomson, D. J. (2016). Analytical solutions of the supersaturation equation for a warm cloud. *Journal of the Atmospheric Sciences*, *73*(9), 3453–3465. https://doi.org/10.1175/JAS-D-15-0281.1

Dinar, E., Taraniuk, I., Graber, E. R., Katsman, S., Moise, T., Anttila, T., Mentel, T. F., & Rudich, Y. (2006). Cloud Condensation Nuclei properties of model and atmospheric HULIS. *Atmospheric Chemistry and Physics*, *6*(9), 2465–2482. https://doi.org/10.5194/acp-6-2465-2006

Ekström, S., Nozière, B., Hultberg, M., Alsberg, T., Magnér, J., Nilsson, E. D., & Artaxo, P. (2010). A possible role of ground-based microorganisms on cloud formation in the atmosphere. *Biogeosciences*, *7*(1), 387–394. https://doi.org/10.5194/bg-7-387-2010

Facchini, M. C., Decesari, S., Mircea, M., Fuzzi, S., Loglio, G., G, L., Facchini, M. C., Decesari, S., Mircea, M., Fuzzi, S., & Loglio, G. (2000). Surface tension of atmospheric wet aerosol and cloud/fog droplets in relation to their organic carbon content and chemical composition. *Atmospheric Environment*, *34*(28), 4853–4857. https://doi.org/10.1016/S1352-2310(00)00237-5

Facchini, M. C., Mircea, M., Fuzzi, S., & Charlson, R. J. (1999). Cloud albedo enhancement by surface-active organic solutes in growing droplets. *Nature*, *401*(6750), 257–259. https://doi.org/10.1038/45758

Floris, R., Rizzo, C., & lo Giudice, A. (2020). Biosurfactants from Marine Microorganisms. In *Metabolomics - New Insights into Biology and Medicine*. Wael N. Hozzein, Editor. IntechOpen, London 2018. https://doi.org/10.5772/intechopen.80493

Frossard, A. A., Gérard, V., Duplessis, P., Kinsey, J. D., Lu, X., Zhu, Y., Bisgrove, J., Maben, J. R., Long, M. S., Chang, R. Y. W., Beaupré, S. R., Kieber, D. J., Keene, W. C., Nozière, B., & Cohen, R. C. (2019). Properties of Seawater Surfactants Associated with Primary Marine Aerosol Particles Produced by Bursting Bubbles at a Model Air-Sea Interface. *Environmental Science and Technology*, *53*(16), 9407–9417. https://doi.org/10.1021/acs.est.9b02637

Gerard, V. (2017). *Surfactants in atmospheric aerosols and their role on cloud formation*. PhD thesis Université de Lyon , 2016

Gérard, V., Kumar Singh, Dharmendra Fine, L., Ferronato, C., Frossard, A. A., Cohen, R. C., Asmi, E., Lihavainen, H., Kivekäs, N., Aurela, M., Brus, D., Frka, S., Kušan, A. C., & Noziere, B. (2019). The Role of Surfactants on Cloud Formation: Surfactants in PM1 Aerosols from Urban

to Remote Regions and Correlations with Cloud Occurrence. *Geophysical Research Abstracts, EGU2019-7898-1*.

Gérard, V., Noziere, B., Fine, L., Ferronato, C., Singh, D. K., Frossard, A. A., Cohen, R. C., Asmi, E., Lihavainen, H., Kivekäs, N., Aurela, M., Brus, D., Frka, S., & Cvitešić Kušan, A. (2019). Concentrations and Adsorption Isotherms for Amphiphilic Surfactants in PM 1 Aerosols from Different Regions of Europe. *Environmental Science & Technology*, *53*(21), 12379–12388. https://doi.org/10.1021/acs.est.9b03386

Hyttinen, N., Elm, J., Malila, J., Calderón, S. M., & Prisle, N. L. (2020a). Thermodynamic properties of isoprene- and monoterpene-derived organosulfates estimated with COSMO *Atmospheric Chemistry and Physics*, *20*(9), 5679–5696. https://doi.org/10.5194/acp-20-5679-2020

IPCC. (2014). *IPCC, 2014: Climate Change 2014: Synthesis Report. Contribution of Working Groups I, II and III to the Fifth Assessment Report of the Intergovernmental Panel on Climate Change [Core Writing Team* (R. K. P. and L. A. M. (eds)]). IPCC Geneva, Switzerland, 151 pp..

IPCC, Masson-Delmotte, V., Zhai, P., Pirani, A., Connors, S. L., Péan, C., Berger, S., Caud, N., Chen, Y., Goldfarb, L., Gomis, M. I., Huang, M., Leitzell, K., Lonnoy, E., Matthews, J. B. R., Maycock, T. K., Waterfield, T., Yelekçi, O., Yu, R., & B., Z. (2021). Climate Change 2021: The Physical Science Basis. Contribution of Working Group I to the Sixth Assessment Report of the Intergovernmental Panel on Climate Change. *Cambridge University Press*, *In Press*,

Janz, G. (1988). Thermodynamic and Transport Properties for molten salts, correlated equations for critically evaluated density, surface tension, electrical conductance and viscosity data. *Journal of Physical and Chemical Reference Data*, *17*(Supp. No. 2), 1–320.

Kaluarachchi, C. P., Or, V. W., Lan, Y., Madawala, C. K., Hasenecz, E. S., Crocker, D. R., Morris, C. K., Lee, H. D., Mayer, K. J., Sauer, J. S., Lee, C., Dorce, G., Malfatti, F., Stone, E. A., Cappa, C. D., Grassian, V. H., Prather, K. A., & Tivanski, A. V. (2022a). Size-Dependent Morphology, Composition, Phase State, and Water Uptake of Nascent Submicrometer Sea Spray Aerosols during a Phytoplankton Bloom. *ACS Earth and Space Chemistry*, *6*(1), 116–130. https://doi.org/10.1021/acsearthspacechem.1c00306

Kasparian, J., Hassler, C., Ibelings, B., Berti, N., Bigorre, S., Djambazova, V., Gascon-Diez, E., Giuliani, G., Houlmann, R., Kiselev, D., De Laborie, P., Le, A. D., Magouroux, T., Neri, T., Palomino, D., Pfändler, S., Ray, N., Sousa, G., Staedler, D., … Beniston, M. (2017). Assessing the Dynamics of Organic Aerosols over the North Atlantic Ocean. *Scientific Reports*, *7*, 1–10. https://doi.org/10.1038/srep45476

Kirpes, R. M., Bonanno, D., May, N. W., Fraund, M., Barget, A. J., Moffet, R. C., Ault, A. P., & Pratt, K. A. (2019). Wintertime Arctic Sea Spray Aerosol Composition Controlled by Sea Ice Lead Microbiology. *ACS Central Science*, *5*(11), 1760–1767. https://doi.org/10.1021/acscentsci.9b00541

Kiss, G., Tombácz, E., & Hansson, H. C. (2005). Surface tension effects of humic-like substances in the aqueous extract of tropospheric fine aerosol. *Journal of Atmospheric Chemistry*, *50*(3), 279–294. https://doi.org/10.1007/s10874-005-5079-5

Köhler, H. (1936). The nucleus in and the growth of hygroscopic droplets. *Transactions of the Faraday Society*, *32*(1152), 1152–1161. https://doi.org/10.1039/TF9363201152

Kristensson, A., Rosenørn, T., & Bilde, M. (2010a). Cloud droplet activation of amino acid aerosol particles. *Journal of Physical Chemistry A*, *114*(1), 379–386. https://doi.org/10.1021/jp9055329

Kristensson, A., Rosenørn, T., & Bilde, M. (2010b). Cloud droplet activation of amino acid aerosol particles. *Journal of Physical Chemistry A*, *114*(1), 379–386. https://doi.org/10.1021/jp9055329

Kroflič, A., Frka, S., Simmel, M., Wex, H., & Grgić, I. (2018). Size-Resolved Surface-Active Substances of Atmospheric Aerosol: Reconsideration of the Impact on Cloud Droplet Formation. *Environmental Science and Technology*, *52*(16), 9179–9187. https://doi.org/10.1021/acs.est.8b02381

Langevin, D. (1992a). Micelles and Microemulsions. *Annual Review of Physical Chemistry*, *43*(1), 341–369. https://doi.org/10.1146/annurev.pc.43.100192.002013

Langevin, D. (1992b). Micelles and Microemulsions. *Annual Review of Physical Chemistry*, *43*(1), 341–369. https://doi.org/10.1146/annurev.pc.43.100192.002013

Lawler, M. J., Lewis, S. L., Russell, L. M., Quinn, P. K., Bates, T. S., Coffman, D. J., Upchurch, L. M., & Saltzman, E. S. (2020). North Atlantic marine organic aerosol characterized by novel offline thermal desorption mass spectrometry: polysaccharides, recalcitrant material, and secondary organics. *Atmospheric Chemistry and Physics*, *20*(24), 16007–16022. https://doi.org/10.5194/acp-20-16007-2020

Li, W., Sun, J., Xu, L., Shi, Z., Riemer, N., Sun, Y., Fu, P., Zhang, J., Lin, Y., Wang, X., Shao, L., Chen, J., Zhang, X., Wang, Z., & Wang, W. (2016). A conceptual framework for mixing structures in individual aerosol particles. *Journal of Geophysical Research: Atmospheres*, *121*(22), 13,713-784,798. https://doi.org/10.1002/2016JD025252

Li, X., Hede, T., Tu, Y., Leck, C., & Gren, H. Å. (2013). Cloud droplet activation mechanisms of amino acid aerosol particles: Insight from molecular dynamics simulations. *Tellus, Series B: Chemical and Physical Meteorology*, *65*(1). https://doi.org/10.3402/tellusb.v65i0.20476

Li, Z., Williams, A. L., Rood, M. J., Li, Z., Williams, A. L., & Rood, M. J. (1998). Influence of Soluble Surfactant Properties on the Activation of Aerosol Particles Containing Inorganic Solute. *Journal of the Atmospheric Sciences*, *55*(10), 1859–1866. https://doi.org/10.1175/1520-0469(1998)055<1859:IOSSPO>2.0.CO;2

Lin, J. J., Malila, J., & Prisle, N. L. (2018). Cloud droplet activation of organic-salt mixtures predicted from two model treatments of the droplet surface. *Environmental Science: Processes and Impacts*, *20*(11), 1611–1629. https://doi.org/10.1039/c8em00345a

Liu, L., Kong, S., Zhang, Y., Wang, Y., Xu, L., Yan, Q., Lingaswamy, A. P., Shi, Z., Lv, S., Niu, H., Shao, L., Hu, M., Zhang, D., Chen, J., Zhang, X., & Li, W. (2017). Morphology, composition, and mixing state of primary particles from combustion sources — crop residue, wood, and solid waste. *Scientific Reports*, *7*(1), 5047. https://doi.org/10.1038/s41598-017-05357-2

Malila, J., & Prisle, N. L. (2018). A Monolayer Partitioning Scheme for Droplets of Surfactant Solutions. *Journal of Advances in Modeling Earth Systems*, *10*(12), 3233–3251. https://doi.org/10.1029/2018MS001456

Mayer, K. J., Wang, X., Santander, M. V., Mitts, B. A., Sauer, J. S., Sultana, C. M., Cappa, C. D., & Prather, K. A. (2020a). Secondary Marine Aerosol Plays a Dominant Role over Primary Sea Spray Aerosol in Cloud Formation. *ACS Central Science*, *6*(12), 2259–2266. https://doi.org/10.1021/acscentsci.0c00793

Mayer, K. J., Wang, X., Santander, M. V., Mitts, B. A., Sauer, J. S., Sultana, C. M., Cappa, C. D., & Prather, K. A. (2020b). Secondary Marine Aerosol Plays a Dominant Role over Primary Sea Spray Aerosol in Cloud Formation. *ACS Central Science*, *6*(12), 2259–2266. https://doi.org/10.1021/acscentsci.0c00793

Mochida, M., Kitamori, Y., Kawamura, K., Nojiri, Y., & Suzuki, K. (2002). Fatty acids in the marine atmosphere: Factors governing their concentrations and evaluation of organic films on sea-salt particles. *Journal of Geophysical Research Atmospheres*, *107*(17), AAC 1-1-AAC 1-10. https://doi.org/10.1029/2001JD001278

Morales Betancourt, R., & Nenes, A. (2014). Droplet activation parameterization: The population-splitting concept revisited. *Geoscientific Model Development*, *7*(5), 2345–2357. https://doi.org/10.5194/gmd-7-2345-2014

Nenes, A., Ghan, S., Abdul-Razzak, H., Chuang, P. Y., & Seinfeld, J. H. (2001). Kinetic limitations on cloud droplet formation and impact on cloud albedo. *Tellus B: Chemical and Physical Meteorology*, *53*(2), 133–149. https://doi.org/10.3402/tellusb.v53i2.16569

Nenes, A., & Seinfeld, J. H. (2003). Parameterization of cloud droplet formation in global climate models. *Journal of Geophysical Research: Atmospheres*, *108*(D14). https://doi.org/https://doi.org/10.1029/2002JD002911

Nozière, B., Gérard, V., Baduel, C., & Ferronato, C. (2017a). Extraction and Characterization of Surfactants from Atmospheric Aerosols. *JoVE*, *122*, e55622. https://doi.org/doi:10.3791/55622

O'Dowd, C. D., Facchini, M. C., Cavalli, F., Ceburnis, D., Mircea, M., Decesari, S., Fuzzi, S., Yoon, Y. J., & Putaud, J.-P. (2004). Biogenically driven organic contribution to marine aerosol. *Nature*, *431*(7009), 676–680. https://doi.org/10.1038/nature02959

Ogunro, O. O., Burrows, S. M., Elliott, S., Frossard, A. A., Hoffman, F., Letscher, R. T., Moore, J. K., Russell, L. M., Wang, S., & Wingenter, O. W. (2015). Global distribution and surface activity of macromolecules in offline simulations of marine organic chemistry. *Biogeochemistry*, *126*(1–2), 25–56. https://doi.org/10.1007/s10533-015-0136-x

Oppo, C., Bellandi, S., Degli Innocenti, N., Stortini, A. M., Loglio, G., Schiavuta, E., & Cini, R. (1999). Surfactant components of marine organic matter as agents for biogeochemical fractionation and pollutant transport via marine aerosols. *Marine Chemistry*, *63*(3), 235–253. https://doi.org/https://doi.org/10.1016/S0304-4203(98)00065-6

Ovadnevaite, J., Zuend, A., Laaksonen, A., Sanchez, K. J., Roberts, G., Ceburnis, D., Decesari, S., Rinaldi, M., Hodas, N., Facchini, M. C., Seinfeld, J. H., & O' Dowd, C. (2017). Surface tension prevails over solute effect in organic-influenced cloud droplet activation. *Nature*, *546*(7660), 1–5. https://doi.org/10.1038/nature22806

Pátek, J., Hrub, J., Klomfar, J., Součková, M., & Harvey, A. H. (2009). Reference correlations for thermophysical properties of liquid water at 0.1 MPa. *Journal of Physical and Chemical Reference Data*, *38*(1), 21–29. https://doi.org/10.1063/1.3043575

Pegram, L. M., & Record, M. T. (2007). Hofmeister salt effects on surface tension arise from partitioning of anions and cations between bulk water and the air-water interface. *Journal of Physical Chemistry B*, *111*(19), 5411–5417. https://doi.org/10.1021/jp070245z

Petrova, T., & Dooley, R. B. (2014). Revised Release on the Surface Tension of Ordinary Water Substance. *Proceedings of the International Association for the Properties of Water and Steam*, *76*(June), 23–27. http://www.iapws.org

Petters, M. D., & Kreidenweis, S. M. (2007). A single parameter representation of hygroscopic growth and cloud condensation nucleus activity. *Atmospheric Chemistry and Physics*, *7*(8), 1961–1971. https://doi.org/10.5194/acp-7-1961-2007

Prisle, N. L., Raatikainen, T., Laaksonen, A., & Bilde, M. (2010). Surfactants in cloud droplet activation: mixed organic-inorganic particles. *Atmospheric Chemistry and Physics*, *10*(12), 5663–5683. https://doi.org/10.5194/acp-10-5663-2010

Prisle, N. L., Raatikainen, T., Sorjamaa, R., Svenningsson, B., Laaksonen, A., & Bilde, M. (2008). Surfactant partitioning in cloud droplet activation: a study of C8, C10, C12 and C14 normal fatty acid sodium salts. *Tellus B: Chemical and Physical Meteorology*, *60*(3), 416–431. https://doi.org/10.1111/j.1600-0889.2008.00352.x

Quinn, P. K., Coffman, D. J., Johnson, J. E., Upchurch, L. M., & Bates, T. S. (2017). Small fraction of marine cloud condensation nuclei made up of sea spray aerosol. *Nature Geoscience*, *10*(9), 674–679. https://doi.org/10.1038/ngeo3003

Quinn, P. K., Collins, D. B., Grassian, V. H., Prather, K. A., & Bates, T. S. (2015). Chemistry and Related Properties of Freshly Emitted Sea Spray Aerosol. *Chemical Reviews*, *115*(10), 4383–4399. https://doi.org/10.1021/cr500713g

Renard, P., Canet, I., Sancelme, M., Matulova, M., Uhliarikova, I., Eyheraguibel, B., Nauton, L., Devemy, J., Traïkia, M., Malfreyt, P., & Delort, A.-M. (2019). Cloud Microorganisms, an Interesting Source of Biosurfactants. *Surfactants and Detergents*, 1–17.

Renard, P., Canet, I., Sancelme, M., Wirgot, N., Deguillaume, L., & Delort, A.-M. (2016). Screening of cloud microorganisms isolated at the Puy de Dôme (France) station for the production of

biosurfactants. *Atmospheric Chemistry and Physics*, *16*(18), 12347–12358. https://doi.org/10.5194/acp-16-12347-2016

Romsted, L. S. (2012). Introduction to Surfactant Self-Assembly. *Supramolecular Chemistry*. https://doi.org/10.1002/9780470661345.smc013

Sareen, N., Schwier, A. N., Lathem, T. L., Nenes, A., & McNeill, V. F. (2013). Surfactants from the gas phase may promote cloud droplet formation. *Proceedings of the National Academy of Sciences*, *110*(8), 2723–2728. https://doi.org/10.1073/pnas.1204838110

Schiffer, J. M., Mael, L. E., Prather, K. A., Amaro, R. E., & Grassian, V. H. (2018). Sea Spray Aerosol: Where Marine Biology Meets Atmospheric Chemistry. *ACS Central Science*, *4*(12), 1617–1623. https://doi.org/10.1021/acscentsci.8b00674

Seinfeld, J. H., & Pandis, S. N. (1998a). Atmospheric Chemistry and Physics: From Air Pollution to Climate Change. In *Environment: Science and Policy for Sustainable Development,* London (3rd ed.. John Wiley and Sons, Inc. https://doi.org/10.1080/00139157.1999.10544295

Shinoda, K., & Hutchinson, E. (1962). Pseudo-phase separation model for thermodynamic calculations on micellar solutions. *Journal of Physical Chemistry*, *66*(4), 577–582. https://doi.org/10.1021/j100810a001

Sorjamaa, R., Svenningsson, B., Raatikainen, T., Henning, S., Bilde, M., & Laaksonen, A. (2004). The role of surfactants in Köhler theory reconsidered. *Atmospheric Chemistry and Physics*, *4*(8), 2107–2117. https://doi.org/10.5194/acp-4-2107-2004

Stephanou, E. G. (1992). Biogenic and anthropogenic organic compounds in eolian particulates in the East Mediterranean region-I. Occurrence and origin. *Atmospheric Environment Part A, General Topics*, *26*(15), 2821–2829. https://doi.org/10.1016/0960-1686(92)90019-H

Tharwat, F. T. (2014). *An Introduction to Surfactants* (1st ed.). Berlin: De Gruyter.

Vinš, V., Hykl, J., & Hrubý, J. (2019). Surface tension of seawater at low temperatures including supercooled region down to – 25 °C. *Marine Chemistry*, *213*, 13–23. https://doi.org/10.1016/j.marchem.2019.05.001

Wang, X., Deane, G. B., Moore, K. A., Ryder, O. S., Stokes, M. D., Beall, C. M., Collins, D. B., Santander, M. V, Burrows, S. M., Sultana, C. M., & Prather, K. A. (2017). The role of jet and film drops in controlling the mixing state of submicron sea spray aerosol particles. *Proceedings of the National Academy of Sciences*, *114*(27), 6978–6983. https://doi.org/10.1073/pnas.1702420114

Weast, R. C. (ed). (1989a). CRC handbook of chemistry and physics. In *Biochemical Education*. Taylor & Francis, London. https://doi.org/10.1016/0307-4412(89)90022-8